

FMH606 Master's Thesis 2024
Process Technology

The use of inert gas for mitigating fires and gas explosions

Charith Rajapaksha

The University of South-Eastern Norway takes no responsibility for the results and conclusions in this student report.

Course: FMH606 Master's Thesis, 2024

Title: The Use of Inert Gas for Mitigating Fires and Gas Explosions

Number of pages: 60

Keywords: Inergen, Hydrogen safety, Li-ion battery gas safety, Gas explosions, Maximum explosion pressure, Maximum rate of explosion pressure rise, Premixed combustion, Cantera, Inert gases, Fire safety

Student: Charith Rajapaksha

Supervisor: Prof. Dag Bjerketvedt and Assistant prof. Mathias Henriksen

External partner: Equinor and MoZEES

Summary:

Hydrogen has been proposed as an alternative carbon-zero energy source for power generation fuel cells, transportation, and other industries. Furthermore, Li-ion batteries are gaining popularity as a better storage storage for converted green energy because they have higher energy density and low maintenance costs. However, both hydrogen and Li-ion batteries pose a significant fire hazard. Hydrogen is regarded as a very flammable substance with its properties, and Li-ion batteries, known as thermal runaway, can vent out flammable gas mixtures in case of failure. A significant number of incidents have been reported and will increase with the increasing demand for hydrogen and Li-ion batteries. Therefore, understanding this behaviour and implementing safety barriers for hydrogen and lithium-ion battery-vented gas is essential. Adding an inert gas to a flammable mixture is one of the steps that can be taken to avoid an undesirable consequence like a fire or an explosion.

This work studied combustion characteristics of hydrogen and li-ion battery-vented gases with air and inergen mixtures in a 20-litre explosion sphere vessel at 300 K and 1 atm absolute pressure. Maximum explosion pressure, maximum rate of explosion pressure rise, and deflagration index were measured for different mixture compositions. A simple flammability limit analysis was done on hydrogen-air-inergen mixtures to identify how inergen affects the flammability of hydrogen. A comparison was done to validate the experimental results with numerical calculations based on Cantera and experimental data with other published research results.

Hydrogen and air mixtures agreed well with the computational results and the published data. Hydrogen showed better combustion characteristics than battery gases used in the experiments. However, with the inclusion of inergen, deviations were observed between the actual and the computational results. The results showed that adding inergen to a flammable mixture significantly reduces its flammable properties.

The University of South-Eastern Norway takes no responsibility for the results and conclusions in this student report.

Preface

This master's thesis shows the research work carried out in the spring of 2024 at the University of South-Eastern Norway (USN), Porsgrunn. This research work and thesis are being conducted as part of the requirement for the Master of Science degree at USN. This thesis was supervised by Prof. Dag Bjerketvedt and Associate Professor Mathias Henriksen, with whom I have learned and broadened my knowledge and skills immensely during this thesis.

First and foremost, I would like to express my sincere gratitude and appreciation to Prof. Dag Bjerketvedt and Associate Professor Mathias Henriksen, who guided me throughout the thesis. I want to thank them for their valuable time spent evaluating my work and giving me valuable advice. I am grateful to them for all the academic knowledge and techniques I learned during my work.

I would also like to thank the dedicated staff at the USN library for their consistent assistance whenever needed. Furthermore, I am grateful to Equinor and MoZEES for allowing young professionals to learn and gain knowledge in the industry so we can shape the future.

Finally, I would like to thank my friends and family, who constantly encouraged and supported me in doing my best to complete the thesis.

Porsgrunn, 14.05.2024

Charith Rajapaksha

Abbreviations

LIB	Lithium-ion battery
LBV	Laminar burning velocity
LEL	Lower explosion limit
UEL	Upper explosion limit
LFL	Lower flammability limit
UFL	Upper flammability limit
RFL	Richer flammability limit
SOC	State of charge
HIAD	Hydrogen Incidents and Accidents Database
FT	Flame temperature
MIC	Minimum inerting concentration
LOC	Limiting oxygen concentration
IG100	Nitrogen
IG01	Argon
IG541	Inergen
IG55	Argonite
NOAEL	No observable adverse effects level
LOAEL	Lowest observable adverse effects level
ODP	Ozone-depleting potential
GWP	Global warming potential
LED	Light emitting diode
atm	Atmosphere
BG	Battery gas
NFPA	National Fire Protection Agency

Nomenclature

Symbol	Description	Units
$(P_{ex})_{max}$	Maximum explosion pressure	kPa
$(dp/dt)_{max}$	Maximum rate of explosion pressure rise	MPa/s
ϕ	Equivalence ratio	-
S_u	Laminar burning velocity	m/s
K_G	Deflagration index	bar.m/s
V	Volume	m ³
P_o	Initial pressure	kPa
phi	Equivalence ratio	-
$X_{inergen}$	Mole fraction of inergen	-
T_{ad}	Adiabatic temperature	K

Table of contents

Preface	I
Nomenclature	III
Table of contents.....	IV
Table of Figures.....	VI
1 Introduction	1
1.1 Objectives.....	2
1.2 Thesis Structure.....	2
2 Theory and literature review	3
2.1 Premixed flame	3
2.2 Laminar burning velocity	3
2.3 Flammability limits.....	4
2.4 Factors affecting flammability	5
2.4.1 <i>Temperature and Pressure</i>	5
2.4.2 <i>Fuel and oxidiser concentration</i>	6
2.5 Maximum explosion pressure ($(P_{ex})_{max}$)	6
2.6 Maximum rate of pressure rise $(dp/dt)_{max}$	6
2.7 Deflagration index (KG).....	7
2.8 Hydrogen Fire Safety Overview.....	7
2.9 Lithium-ion battery fire safety overview	9
2.10 Overview of Inert Gas Technology	9
2.10.1 <i>Inert gas system</i>	10
2.10.2 <i>Common inert gases used in fire suppression</i>	11
2.10.3 <i>Inergen as a fire suppressant inert gas</i>	11
2.11 Related work done.....	13
3 Methodology.....	18
3.1 Experimental setup.....	18
3.1.1 <i>Materials used</i>	19
3.1.2 <i>Procedure of experiment</i>	20
3.1.3 <i>Maximum explosion pressure and maximum rate of explosion pressure rise</i>	20
3.1.4 <i>Maximum rate of explosion pressure rise</i>	20
3.2 Cantera Numerical calculation	21
3.2.1 <i>Maximum explosion pressure</i>	21
3.2.2 <i>Flammability limit approximation</i>	21
4 Results.....	23
4.1 Maximum explosion pressure	23
4.1.1 <i>Hydrogen combustion with inergen</i>	23
4.1.2 <i>Battery gas combustion with inergen</i>	24
4.1.3 <i>Maximum explosion pressure ratio $P_{ex}P_o$</i>	25
4.2 $(dp/dt)_{max}$ values and KG values	27
4.2.1 <i>Maximum rate of explosion pressure rise</i>	27
4.2.2 <i>Deflagration index (KG) values</i>	28
4.3 Simple flammability limits analysis	29
4.3.1 <i>Hydrogen flammability</i>	29
5 Discussion.....	31

5.1 Validation of experimental results	31
5.1.1 <i>Comparing experimental values with the literature</i>	31
5.1.2 <i>Comparing experimental values with the simulated values</i>	32
5.2 Maximum explosion pressure	32
5.3 Maximum rate of explosion pressure rise.....	33
5.4 How inergen affects the oxygen concentration.....	34
5.5 Approximated flammability levels at the NOAEL and LOAEL.....	35
6 Future work	37
7 Conclusion	38
References	39
Appendices	42

Table of Figures

FIGURE 1.1: GLOBAL HYDROGEN DEMAND PROJECTION WITH ITS APPLICATION. [2].....	1
FIGURE 1.2: LI-ION BATTERY DEMAND FORECAST [5].....	1
FIGURE 2.1: STRUCTURE OF PREMIXED FLAME STRUCTURE [9].	3
FIGURE 2.2: RELATIONSHIP BETWEEN FLAMMABILITY PROPERTIES [16].....	4
FIGURE 2.3: INFLUENCE OF THE TEMPERATURE ON THE FLAMMABILITY LIMITS [20]	5
FIGURE 2.4: FLAMMABLE RANGE HYDROGEN-AIR AT VARIOUS PRESSURES [15] [21]	6
FIGURE 2.5: P_{max} AND $(dp/dt)_{max}$ [23]	7
FIGURE 2.6: FLOW CHART OF HAZARD OCCURRENCE DUE TO HYDROGEN LEAKAGE [1].....	8
FIGURE 2.7: OUTCOMES OF ACCIDENTS RELATED TO HYDROGEN [25].....	8
FIGURE 2.8: FLOW CHART INCLUDING FACTORS AFFECTING LIB SAFETY AND CONSEQUENCES OF THEM [27].....	9
FIGURE 2.9: ILLUSTRATION OF DIFFERENT EXTINGUISHMENT WORKING MECHANISMS [3]	10
FIGURE 2.10: METHANE FLAMMABILITY PROPERTIES WITH NITROGEN DILUTION (25 °C AND 1 ATM) [28].	11
FIGURE 2.11: FLAMMABILITY DIAGRAM FOR HYDROGEN/AIR/NITROGEN AT 293 K AND 1 BAR [29]	11
FIGURE 2.12: MAXIMUM EXPLOSION PRESSURE AND EQUILIBRIUM PRESSURE OF HYDROGEN-AIR MIXTURE [36]	13
FIGURE 2.13: EXPERIMENTAL AND COMPUTATIONAL RESULT OF H ₂ -AIR MIXTURE EXPLOSION PRESSURE (LEFT) AND EXPERIMENTAL RESULTS OF H ₂ -AIR MAXIMUM DP/DT VALUES (RIGHT) AT 100 KPA AND 300 K [37]	14
FIGURE 2.14: COMPARISON OF EXPERIMENTAL AND CALCULATED FLAMMABILITY LIMITS FOR PROPANE-N ₂ -AIR MIXTURES (LEFT) AND ETHYLENE-N ₂ -AIR MIXTURES (RIGHT) AT 25 °C AND 1 ATM.	14
FIGURE 2.15: HYDROGEN-AIR EXPLOSION PRESSURE VARIATIONS AT VARIOUS (A) EQUIVALENCE RATIOS, (B) INERT GASES AND (C) INITIAL PRESSURES [39].....	15
FIGURE 2.16: MAXIMUM PRESSURE RISE RATE AND DEFLAGRATION INDEX WITH VARIOUS INERT DILUTIONS [39].	15
FIGURE 2.17: LITHIUM-ION BATTERY COMBUSTION TEMPERATURE CHANGE IN AIR (UPPER LEFT), N ₂ (UPPER RIGHT) AND CO ₂ (LOWER) [40].	16
FIGURE 2.18: OBSERVED (POINTS) AND CALCULATED FLAMMABILITY LIMITS (DASHED LINES) OF METHANE-AIR (LEFT) AND PROPANE-AIR (RIGHT) MIXTURE WITH AGENT A – INERGEN AND AGENT B – ARGONITE [41].	17
FIGURE 3.1: SPHERE BOMB USED IN THE EXPERIMENT.....	18
FIGURE 3.2: SCHEMATIC DIAGRAM OF EXPERIMENTAL SETUP [11]. 1: EXPLOSION CHAMBER; 2: OXIDISER INLET; 3: FLUSH INLET; 4: FUEL (LIQUID) INJECTION PORT; 5: FUEL (GAS) INLET; 6: VACUUM PORT; 7: GAS OUTLET; 8: IGNITION SYSTEM; 9: THERMOCOUPLE; 10: GLASS WINDOWS (100 MM); 11: LED LIGHT SOURCE; 12: HIGH-SPEED CAMERA; 13: STIRRER; 14: HEATING PLATE; 15: AMBIENT TEMPERATURE DISPLAY; 16: DUAL EXPLOSION PRESSURE SENSORS; 17: DATA ACQUISITION SYSTEM; 18: CONTROL/TRIGGER UNIT AND 19: AMBIENT PRESSURE SENSOR.....	19
FIGURE 3.3: PROCESSED RESULT OF A MAXIMUM RATE OF EXPLOSION PRESSURE RISE USING TWO PRESSURE SENSORS.....	21
FIGURE 3.4: MODEL SIMULATION ALGORITHM TO FIND FLAMMABILITY LIMITS.	22
FIGURE 4.1: COMPARISON BETWEEN EXPERIMENTAL AND COMPUTATIONAL RESULTS. LEFT: 'FUEL CONCENTRATION VS. MAXIMUM EXPLOSION PRESSURE' WITH DIFFERENT H ₂ /AIR/INERGEN RATIOS. RIGHT: 'FUEL EQUIVALENCE RATIO VS. MAXIMUM EXPLOSION PRESSURE' WITH DIFFERENT H ₂ /AIR/INERGEN RATIOS AT 300K AND 1 ATM. (A) H ₂ WITH 100% AIR, (B) H ₂ WITH INERGEN 50% + AIR 50% MIXTURE, (C) H ₂ WITH INERGEN 75 % + AIR 25% MIXTURE	24
FIGURE 4.2: COMPARISON BETWEEN EXPERIMENTAL AND COMPUTATIONAL RESULTS FOR BATTERY GASES. 'FUEL EQUIVALENCE RATIO VS MAXIMUM EXPLOSION PRESSURE' WITH DIFFERENT BATTERY GAS/AIR/INERGEN RATIOS AT 300K AND 1 ATM. (A) HIGH LBV BATTERY GAS WITH AIR MIXED WITH 50% INERGEN, (B) HIGH LBV BATTERY GAS WITH AIR MIXED WITH 75% INERGEN, (C) GENERIC BATTERY GAS WITH AIR MIXED WITH 50% INERGEN, (D) GENERIC BATTERY GAS WITH AIR MIXED WITH 75% INERGEN	25
FIGURE 4.3: EXPERIMENTAL RESULT OF 'EQUIVALENCE RATIO – MAXIMUM EXPLOSION PRESSURE RATIO FOR DIFFERENT HYDROGEN MIXTURES AT 300K AND 1 ATM. (A) H ₂ WITH 100% AIR, (B) H ₂ WITH INERGEN 50% + AIR 50% MIXTURE, (C) H ₂ WITH INERGEN 75 % + AIR 25% MIXTURE.	26
FIGURE 4.4: EXPERIMENTAL RESULT OF 'EQUIVALENCE RATIO – MAXIMUM EXPLOSION PRESSURE RATIO FOR DIFFERENT HYDROGEN MIXTURES AT 300K AND 1 ATM. (A) HIGH LBV BATTERY GAS WITH AIR MIXED WITH 50% INERGEN, (B) HIGH LBV BATTERY GAS WITH AIR MIXED WITH 75% INERGEN	26
FIGURE 4.5: EXPERIMENTAL RESULT OF 'PHI – MAXIMUM RATE OF EXPLOSION PRESSURE RISE' WITH DIFFERENT H ₂ /AIR/INERGEN COMPOSITIONS AT 300K AND 1 ATM. (A) H ₂ + (100 % AIR), (B) H ₂ + (50% AIR + 50% INERGEN) (C) H ₂ + (25% AIR + 75% INERGEN).	27

FIGURE 4.6: EXPERIMENTAL RESULT OF 'EQUIVALENCE RATIO – MAXIMUM RATE OF EXPLOSION PRESSURE RISE' WITH BATTERY GASES WITH AIR 50% AND INERGEN 50% MIXTURES. (A) HIGH LBV BATTERY GAS + (50% AIR + 50% INERGEN) (B) GENERIC BATTERY GAS + (50% AIR + 50% INERGEN).	28
FIGURE 4.7: EXPERIMENTAL RESULTS OF 'EQUIVALENCE RATIO – MAXIMUM RATE OF EXPLOSION PRESSURE RISE' WITH ALL THE FUEL MIXTURE TYPES.	28
FIGURE 4.8: EXPERIMENTAL RESULTS OF 'EQUIVALENCE RATIO – DEFLAGRATION INDEX' WITH ALL THE BURNT FUEL MIXTURE TYPES. 29	
FIGURE 4.9: NUMERICAL APPROXIMATION FOR FLAMMABILITY VARIATION FOR HYDROGEN WITH INERGEN ADDED, WITH BURNT AND UNBURNT SAMPLES GIVEN.....	30
FIGURE 5.1: COMPARISON BETWEEN HYDROGEN MAXIMUM EXPLOSION PRESSURE EXPERIMENTAL RESULTS VS. THE RESULTS FOUND FROM LITERATURE AT 300 K AND 1 ATM [36].	31
FIGURE 5.2: FLAMMABILITY VARIATION WITH ADDED INERGEN BETWEEN LITERATURE AND THE PRESENT WORK AT 300 K AND 1 ATM FOR (A) METHANE AND (B) PROPANE [41].	32
FIGURE 5.3: SIMULATED EXPLOSION PRESSURES FOR BATTERY GASES WITH AIR USING CANTERA AT 300 K AND 1 ATM FOR (A) HIGH LBV BATTERY GAS, (B) GENERIC BATTERY GAS	33
FIGURE 5.4: EXPLOSION PRESSURE WITH THE OXYGEN CONCENTRATION AT 1 ATM AND 300 K FOR (A) HYDROGEN WITH 100 AIR, (B) HYDROGEN WITH 50% AIR AND 50% INERGEN, (C) HYDROGEN WITH 25% AIR AND 75 % INERGEN.	35
FIGURE 5.5: STOICHIOMETRIC OXYGEN CONCENTRATION VARIATION WITH INERGEN IN HYDROGEN MIXTURES (LEFT) AND BATTERY GASES (RIGHT) AT 300 K AND 1 ATM.	35
FIGURE 5.6: COMPARISON OF FLAMMABILITY LIMITS APPROXIMATION WITH INERGEN AND THE RECOMMENDED INERGEN CONCENTRATIONS AT 300 K AND 1 ATM FOR (A) HYDROGEN, (B) HIGH LBV BATTERY GAS, AND (C) GENERIC BATTERY GAS... 36	

1 Introduction

The availability of global fossil fuel reserves and increasing global environmental issues like global warming have opened the eyes of humankind to search for a sustainable energy source. Hydrogen has been extensively studied among the proposed alternatives as a carbon-zero energy source. Unlike fossil fuels, it is a clean fuel that produces H₂O as products. Therefore, it has been studied and proposed as a potential energy source combined with fuel cells in power generation, transportation, and other industries [1]. Figure 1.1 illustrates the current global hydrogen demand and the projected hydrogen demand until 2050, which will be around ten times the demand in 2015 [2].

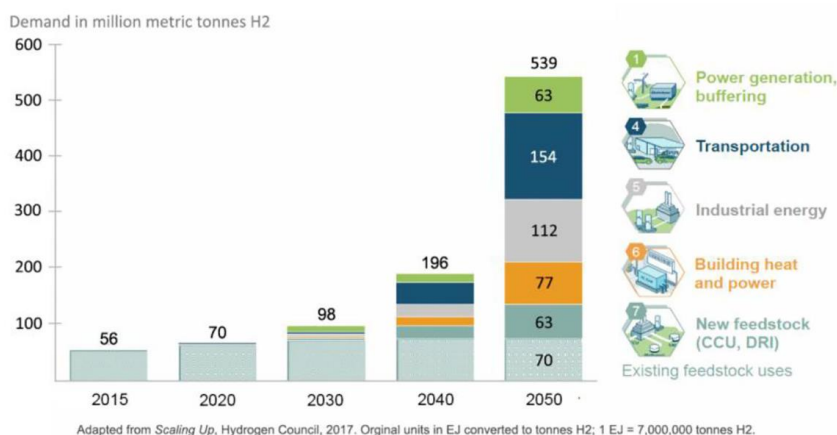


Figure 1.1: Global hydrogen demand projection with its application. [2]

The rapid adoption of renewable energies with the 'net zero 2050' has led to advancements in energy storage technologies, such as lithium-ion batteries (LIB), to store the converted green electric energy until it is used. Figure 1.2 illustrates the projected global LIB demand up to 2030, which is rapidly increasing. Lithium-ion batteries (LIBs) can be used to store energy on a large scale, and they have a higher energy density and low maintenance cost compared to lead-acid, alkaline, and other batteries. LIBs are used in a larger spectrum of applications, from consumer electronics to electric vehicles. A battery cell is the smallest storage unit in a LIB, and multiple battery cells are connected to form a more extensive battery system [3] [4].

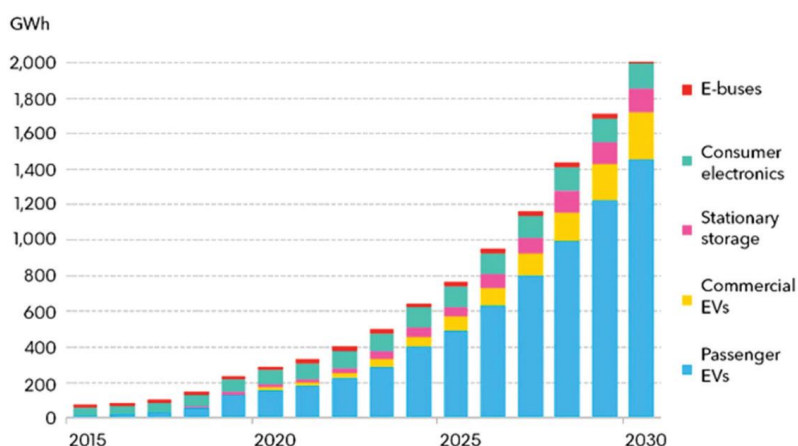


Figure 1.2: Li-ion battery demand forecast [5]

However, using hydrogen as a fuel has several challenges that still need to be answered due to its physical and chemical properties. Furthermore, transporting and storing a substance like hydrogen, which has a wide flammability range (4% - 75 %) and low auto-ignition energy (0.17 mJ for stoichiometric mixture), imposes substantial safety issues [6]. The Bureau for Analysis of Industrial Risks and Pollutions in France reported 177 fire or explosion accidents out of 216 hydrogen-related accidents in their study [7].

Furthermore, although LIBs are growing in popularity, the batteries can fail with two main methods: non-energetic failures, which lead to loss of capacity and energetic failures, which can potentially cause a fire. Several incidents reported batteries catching fires, from small accessories like mobile phones and E-cigarettes to LIB failure in electric buses and aeroplanes [3] [8].

Considering these risks, ensuring safety in environments where hydrogen and battery gases are applied is a critical concern. Therefore, a suitable fire suppression system should be implemented as a safety barrier to avoid such incidents should be implemented. Fire suppressors like water, inert gases, or dry chemicals are used commercially to mitigate fire risks. Inert gases like nitrogen, argon, and carbon dioxide and inert gas mixtures like argonite and inergen are discussed because of their environmentally friendly properties [3]. Therefore, several studies have been carried out on to investigate how adding inert gases to a flammable gas mixture can reduce the likelihood of an ignition.

This study is carried out to examine how hydrogen and battery gas combustion will be affected by mixing the commercialised fire suppression inert gas and inergen into the flammable mixture by running explosion experiments in a 20-L spherical explosion vessel. The obtained explosion results were processed, and the results were compared with Cantera simulation results, and the data obtained from the literature.

1.1 Objectives

- Experimentally measure maximum explosion pressure ($(P_{ex})_{max}$), maximum rate of explosion pressure rise ($(dp/dt)_{max}$) of hydrogen-air-inergen mixtures and vented LIB gases with air-inergen mixtures.
- Calculate the maximum explosion pressure ($(P_{ex})_{max}$), of the selected mixtures numerically.
- Compare the experimental result of explosion pressure with the numerical result and the data from other studies.
- Compare and discuss the flammability of selected fuel-air mixtures with inergen and without inergen.

1.2 Thesis Structure

After the introduction chapter, theories related to premixed combustion, an overview of hydrogen and battery-vented gas safety, and studies relevant to this study are presented in Chapter 2. Chapter 3 discussed the experimental methodology and numerical approach used in Cantera. Chapter 4 shares the obtained experimental results, and Chapter 5 discusses the results in detail. Chapter 6 proposes the future work that can be done with this study and Chapter 7 presents the key findings obtained in the study. Finally, relevant materials not added to the report were added as appendices in the appendix section.

2 Theory and literature review

This chapter is presented mainly in three sub-sections. The first section discusses the theoretical background for understanding premixed combustion and related explosion characteristics. This section covers the fundamental concepts discussed in this study. Secondly, an overview of safety related to hydrogen LIB-vented gases and the combustion characteristics found were discussed. Then, a brief discussion about inergen gas was conducted, including how it works, the human safety factors, and its applications. Finally, a literature review is presented, including studies related to this work.

2.1 Premixed flame

Premixed flames occur in any homogeneous mixture where the fuel and the oxidant are mixed before the reaction. Examples are the Bunsen burner flame and the flame in most spark-ignited engines. The premixed gas is usually expressed in terms of the equivalence ratio (ϕ), the molar ratio of fuel, and the oxidiser to its stoichiometric conditions. Premixed flames can progress either as deflagration or detonation processes [9].

The schematic structure of the premixed flame structure is illustrated in Figure 2.1, and it can be divided into four zones: the unburnt zone, the preheat zone, the reaction zone, and the burned gas zone. The mixture is preheated by the reaction zone in the preheat zone before transferring to the reaction zone where the oxidation occurs.

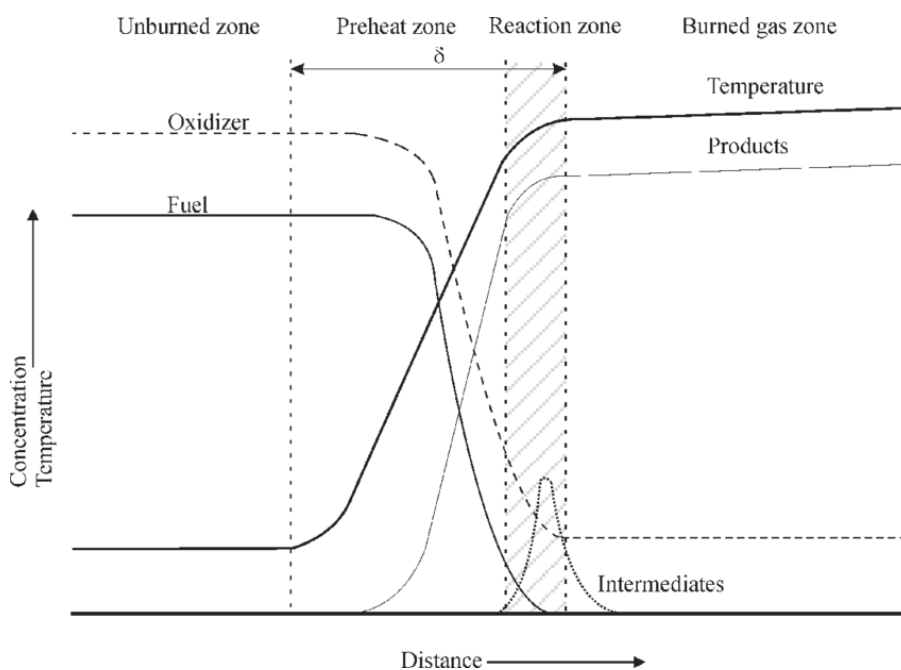


Figure 2.1: Structure of premixed flame structure [9].

2.2 Laminar burning velocity

The laminar burning velocity (S_u) refers to the velocity at which a combustion wave propagates smoothly and orderly compared to the surrounding unburned gas mixture. It is an important

parameter that characterises the propagation of a flat flame into a stationary, unburnt mixture under specific pressure and temperature conditions. S_u mainly depends on the fuel, oxidiser type, fuel-air composition (ϕ), and the temperature of the unburnt premixed mixture. A higher combustion efficiency in fuel with a higher burning velocity can be expected. [9] [10] Table 2.1 presents the (S_u) values of the fuel types used in this study and related fuel types at stoichiometric conditions in ambient temperature and atmospheric pressure.

Table 2.1: Maximum laminar burning velocity of components

Component	Maximum LBV [ms^{-1}]
H ₂	2.91 [10]
CH ₄	0.37 [10]
CO	0.19 [11]
C ₂ H ₄	0.42 [12]
C ₃ H ₈	0.43 [10]
High LBV battery gas	1.05 [13]
Generic battery gas	0.48 [13]

2.3 Flammability limits

Flammability limits of a gas or vapour are defined as the concentration of flammable substance needed in a mixture that can ignite and sustain combustion when exposed to an ignition source [14]. A flammable gas has two flammable limits, namely, lower, and upper flammable limits. The flame speed drops significantly if a fuel mixture gets too rich or lean. Therefore, there are top and bottom limits of equivalence ratio for a fuel mixture where the fuel mixture cannot sustain and propagate a fire.

As in Figure 2.2, a fire or an explosion can only occur when the fuel percentage is between the LEL and UEL. These two limits are referred to as lower explosive limit (LEL)/ lean flammability limit (LFL) and upper explosive limit (UEL)/ rich flammability limit (RFL), respectively, which are usually presented as fuel percentage by volume in the mixture [15].

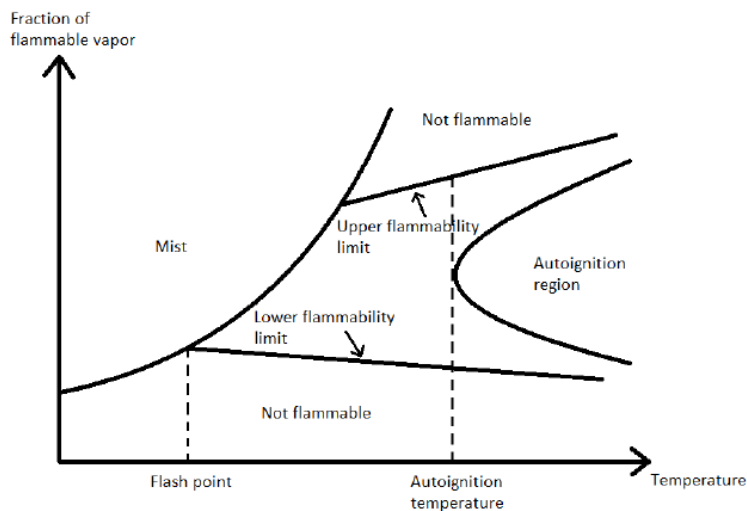


Figure 2.2: Relationship between flammability properties [16]

Table 2.2 reports the flammability limits of the fuel types used in this study and the related fuels at ambient temperature and atmospheric pressure.

Table 2.2: Flammability limits of components at 300 K and 1 atm [17]

Component	Flammability limits
H ₂	4 – 75
CH ₄	4.4 – 16.4
CO	12 – 75
C ₂ H ₄	2.75 – 28.6
C ₃ H ₈	2.1 – 10. 1

For battery-vented gases, a definite range of flammability range was not mentioned because many compositions of battery gases were found. However, they seem to be in a range of 10% LFL and a UFL of around 60% [18].

2.4 Factors affecting flammability

Several factors can affect the flammability ranges of a flammable mixture. The following sub-chapters discuss the main parameters that can affect the flammability limits of a mixture.

2.4.1 Temperature and Pressure

When the temperature increases in a flammable mixture, the limits will widen because the total enthalpy of the initial mixture increases with the temperature. When the mixture temperature is high, the heat required to sustain the flame and continue it to the unburnt fuel portion is reduced, hence the wider flammable region [19]. Figure 2.3 illustrates how temperature variations influenced flammability limits.

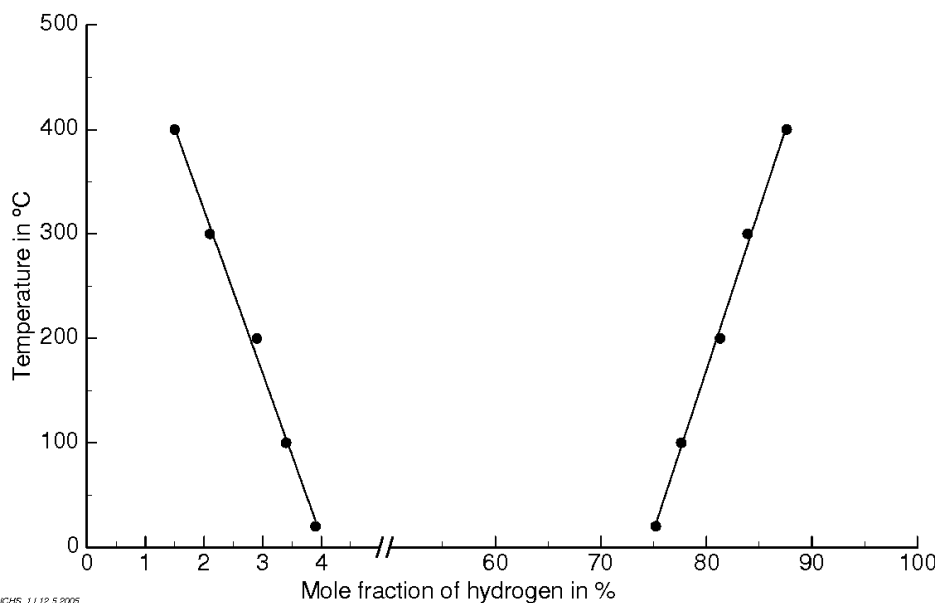


Figure 2.3: Influence of the temperature on the flammability limits [20]

Studies have shown that when the initial pressure and temperature increase, flammable fuel ranges with air are widened. Figure 2.4 illustrates the flammable range widening of hydrogen with initial pressure at a temperature of 21°C and natural gas at 28 °C. According to these, the pressure affects the UFL more than the LFL [15][21].

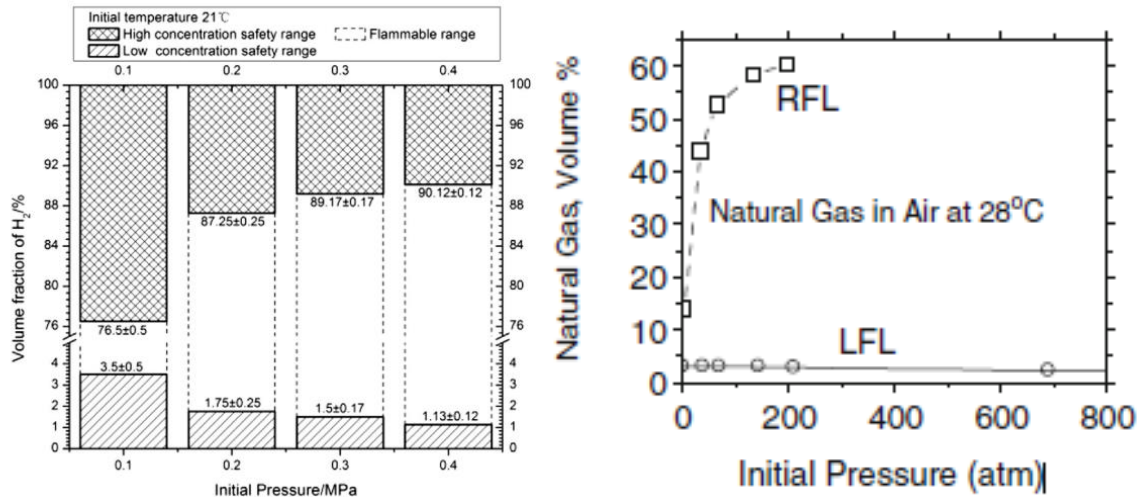


Figure 2.4: Flammable range hydrogen-air at various pressures [15] [21]

2.4.2 Fuel and oxidiser concentration

An oxidiser is a compound that is not necessarily flammable but initiates or promotes combustion through oxidation reactions [22]. Air, including 21% oxygen, is usually used as the oxidiser. A minimum oxygen fraction is required for a flame to propagate. Therefore, reducing the oxidiser fraction in a flammable mixture can also affect its flammability, and this is applied as a safety barrier in industry.

2.5 Maximum explosion pressure ($(P_{ex})_{max}$)

The maximum explosion pressure represents the highest pressure produced during the combustion of a flammable mixture in a confined space, such as a vessel. This pressure increase happens due to the rapid oxidation reaction, which rapidly increases temperature and gas production, resulting in a high-pressure wave, as shown in Figure 2.5. This value is essential to designing safer engineering systems and proper safety barriers. This value can be used to compare the flammability of different mixtures because different mixtures give different maximum explosion pressures. Hydrogen has a maximum explosion pressure of around 6.9 barg, while methane has a value of 7.05 barg at 300 K and 1 atm [16].

2.6 Maximum rate of pressure rise ($(dp/dt)_{max}$)

The maximum pressure rise rate the maximum pressure increases during an explosion, which is the highest gradient in a P_{ex} vs time curve, denoted as $(dp/dt)_{max}$ which indicates the robustness of the explosion. It is influenced by multiple factors, including the properties of the gas mixture, its composition, starting temperature, initial pressure, and vessel volume [16].

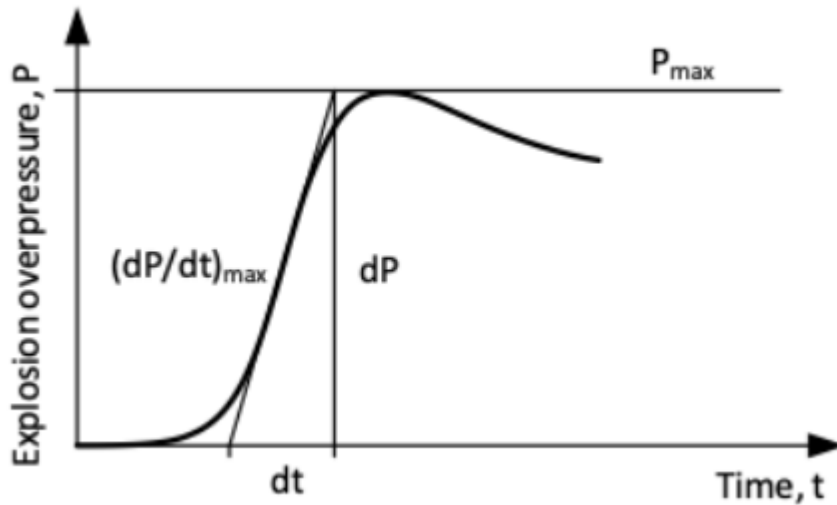


Figure 2.5: P_{max} and $(dp/dt)_{max}$ [23]

2.7 Deflagration index (K_G)

Unlike the maximum explosion pressure and the maximum rate of pressure, the deflagration index represents a fundamental characteristic of the premixed gas. It remains constant regardless of the vessel's volume used in experiments, which makes it easier to compare the intensities of different flammable mixtures in different scenarios [24]. Studies The relationship between K_G and the $\left(\frac{dP}{dt}\right)_{max}$ is shown below in the Equation 2.1 where V is the volume of the combustion vessel.

$$K_G = \left(\frac{dP}{dt}\right)_{max} \times V^{\frac{1}{3}} \quad [2.1]$$

2.8 Hydrogen Fire Safety Overview

Compared to the combustion characteristics, the hydrogen data in chapters 2.2 and 2.3 showed better flammable properties than other flammable gases. Hydrogen has a lower ignition energy and a faster-burning velocity, indicating hydrogen is more prone to catch fire than other substances. Hydrogen has a smaller molar mass, making it more prone to leaks and permeable, and it is an odourless and colourless gas that makes it very difficult to detect. An accidental hydrogen leakage can have dire consequences according to the environment and how it gets leaked. Figure 2.6 illustrates a flow chart of the consequences of a hydrogen leakage, which can end in hazardous incidents like a jet fire or explosion with the space it leaks to and the type of leakage. [1]

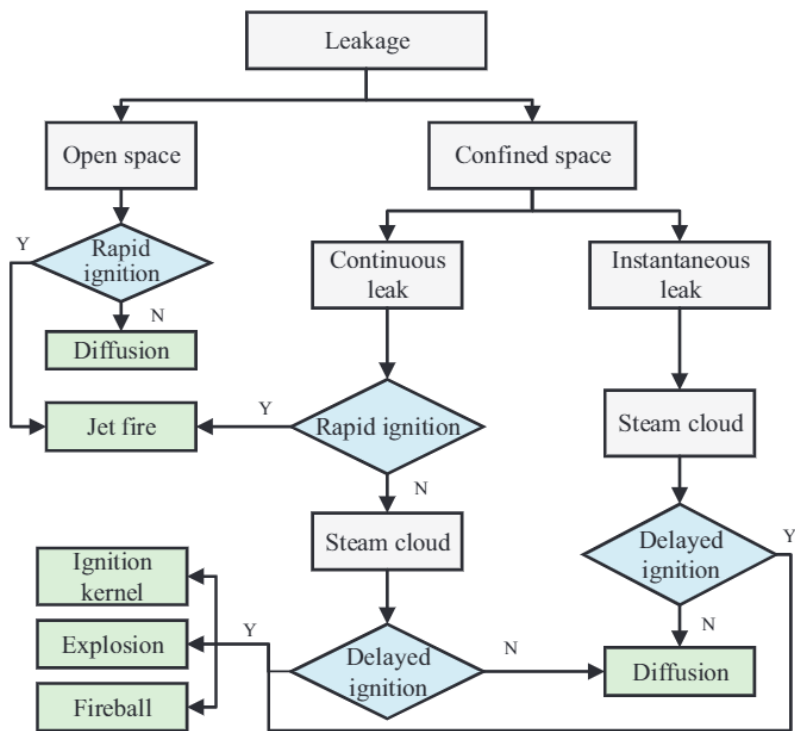


Figure 2.6: Flow chart of hazard occurrence due to hydrogen leakage [1]

Figure 2.7 illustrates the outcome of 576 hydrogen-related accidents until May 2021, recorded in the Hydrogen Incidents and Accidents Database (HIAD) [25]. According to Figure 2.7, around 80% of accidents result in combustion, which is a very high fraction. Therefore, proper fire suppression methods should be implemented when dealing with hydrogen.

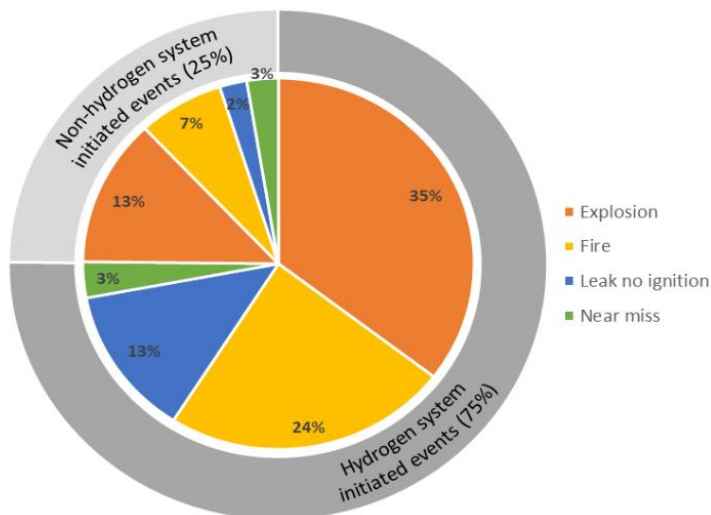


Figure 2.7: Outcomes of accidents related to hydrogen [25]

2.9 Lithium-ion battery fire safety overview

As discussed in the introduction, energetic failure in LIBs can lead to thermal runaway, causing fire. Thermal runaway is one of the main hazards related to LIBs, which can occur due to temperature rise created by uncontrollable exothermic reactions between the cathode, anode, and electrolyte. This can happen when a battery is exposed to thermal, mechanical, and electrical abuse and internal cell faults. In a thermal runaway incident, flammable gases, soot, and metal particles can be vented out from the battery, creating a flammable mixture around the leakage with air readily available for combustion with an ignition source. Even though the probability of a single Li-ion cell failure is very low, with many cells in one battery storage, there can be the possibility that one cell fails and creates dire circumstances, as shown in Figure 2.8 [26].

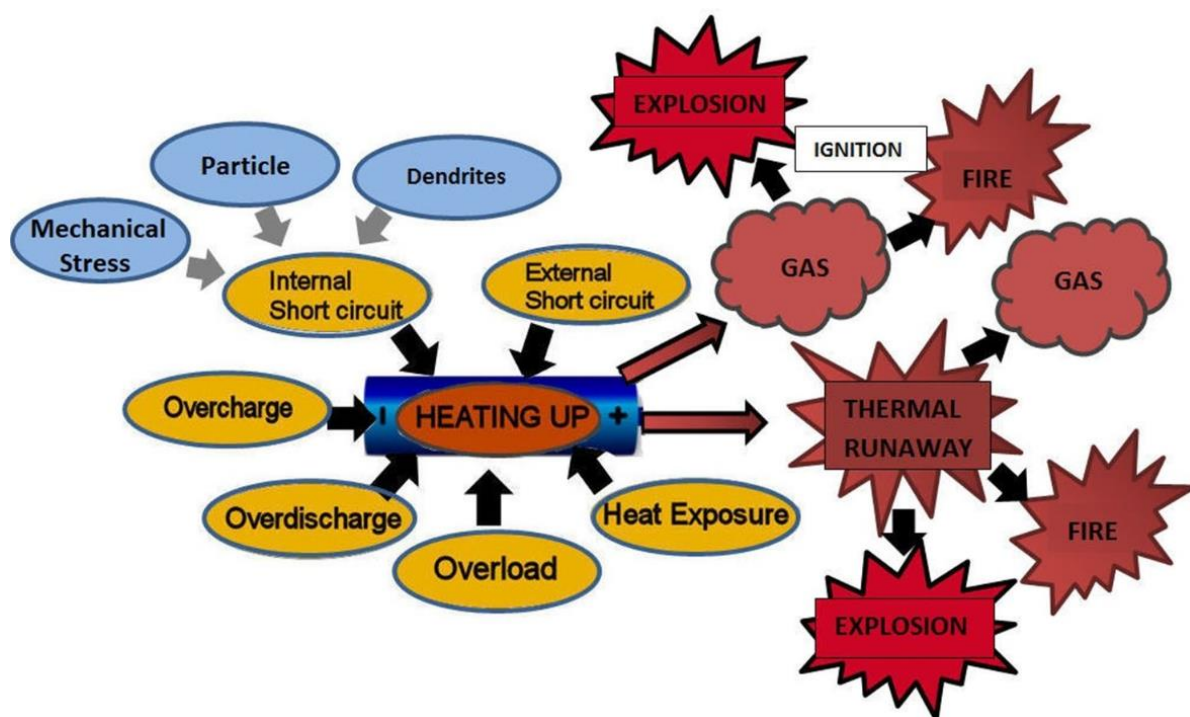


Figure 2.8: Flow chart including factors affecting LIB safety and consequences of them [27]

Several incidents were reported regarding fires that occurred due to LIB failures, from laptops and mobile phones to electric vehicles and large battery pack storage in the industry [3]. Therefore, tackling this issue with better fire suppression systems is vital to avoid catastrophic situations.

2.10 Overview of Inert Gas Technology

As discussed in Chapters 2.09 and 2.10, effective fire suppressions should be deployed to prevent accidents. Many fire suppression systems are available, including water-based sprinkler and water mist systems, gas-based systems with inert gases and powder-based suppression systems. Each fire suppressor has a different mechanism/s to suppress the fire, as illustrated in Figure 2.9 [3].

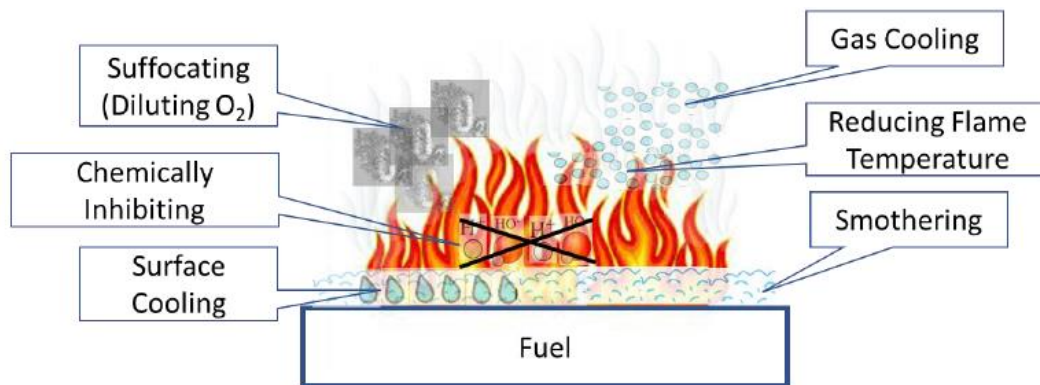


Figure 2.9: Illustration of different extinguishment working mechanisms [3].

Table 2.3 presents an overview of the fire-retardant mechanisms with the fire extinguishing agent and the suppression system.

Table 2.3: Extinguishing mechanism of fire suppression System / extinguishing agent [3].

Suppression system	Working mechanisms
Water-based suppression systems	Cooling, Reducing FT, Suffocating
Gas-based suppression system – Inert gases	Reducing FT, Suffocating
Powder-based suppression system	Chemically inhibiting, Surface cooling
Aerosol systems	Chemically inhibiting, Reducing FT

2.10.1 Inert gas system

It is essential to keep the flammable gases out of the flammable limits or to change their composition to a safer level to prevent combustion. Adding an inert to the combustible mixture to dilute the oxygen level is a widespread technique. Furthermore, adding a substance that does not participate in the combustion process will absorb the heat from the reaction and slow the flame propagation.

Because of these reasons, adding an inert gas to a mixture will narrow the flammability range. When an inert gas is added to the flammable mixture, it reduces the UFL significantly and increases the LFL slowly, as shown in Figure 2.10. As more inert is introduced to the mixture, the UFL and LFL will intersect, and it is known as the minimum inerting concentration point (MIC) since it is the minimum inert needed to ensure that no combustion will occur in the mixture regardless of the hydrogen concentration. Furthermore, the same point is defined as the limiting oxygen concentration (LOC) since no ignition will occur due to insufficient oxygen to propagate a fire [28].

Figure 2.11 illustrates how the flammability limits are influenced by nitrogen in a hydrogen-air mixture. According to Figure 2.7, MIC in H₂/ Air with N₂ seems to be around 75%, and LOC be around 4.5 % [29].

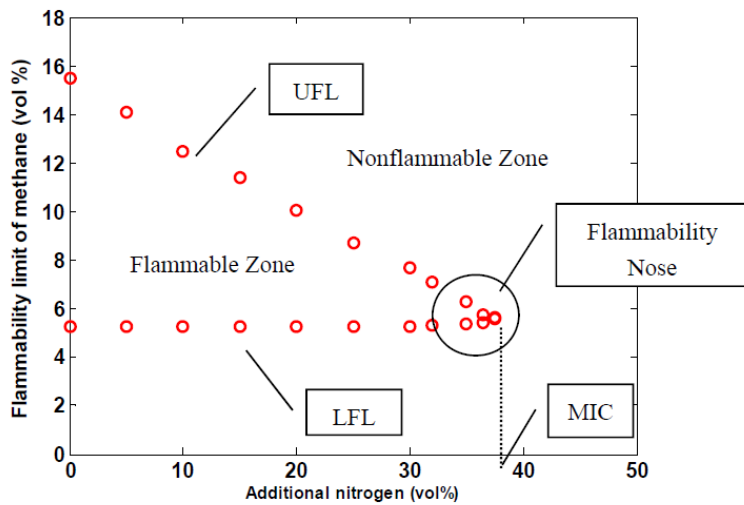


Figure 2.10: Methane flammability properties with nitrogen dilution (25 °C and 1 atm) [28].

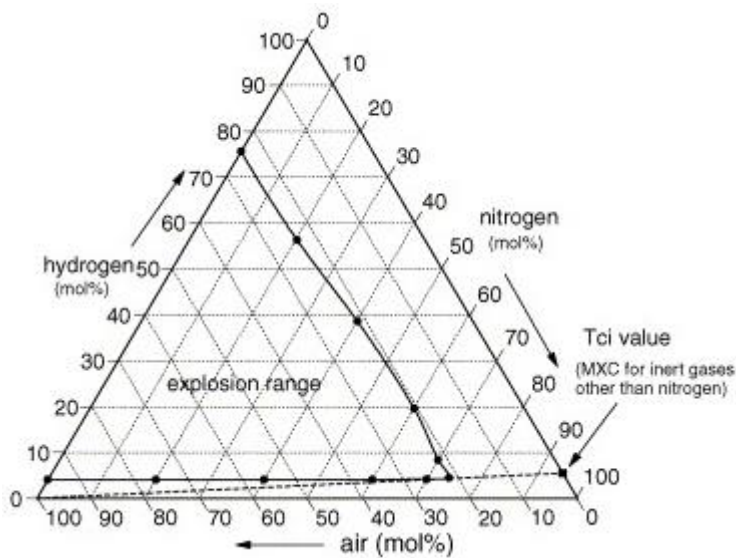


Figure 2.11: Flammability Diagram for Hydrogen/Air/Nitrogen at 293 K and 1 bar [29]

2.10.2 Common inert gases used in fire suppression

Inert gases mainly suppress class A, B and C fire hazards. Commonly used inert gases as fire suppressors are N_2 (IG100), Ar (IG01) and CO_2 . Several studies have found that CO_2 shows better fire suppression than N_2 because of the comparatively higher heat capacity. Furthermore, commercially used inert gas mixtures are also used, including The most used inert gas agents, inergen (IG541) with 52 % N_2 , 40% Ar, 8% CO_2 and argonite (IG55) with 50 % N_2 , 50% Ar [3] [30].

2.10.3 Inergen as a fire suppressant inert gas

Inergen is a commercially used fire suppression agent by Wormald Group, Australia. As discussed in previous chapters, it suppresses fires by oxygen displacement, lowering the atmospheric oxygen level from 21% to an oxygen level that cannot support flame propagation

around 12.5% [31] [32]. There are several factors to assess when to select the suitable inert gas for a system, as discussed in the subtopics below.

2.10.3.1 Fire suppression effectiveness

When evaluating fire suppression agents in terms of their effectiveness, the cup burner concentrations and the minimum design concentration are two main parameters. Cup burner concentration is the minimum concentration of an agent required to extinguish a controlled flame, usually an n-heptane flame, under laboratory conditions. The minimum design concentration is usually around 1.2 times the cup burner concentration. This value is given to achieve the minimum safer concentration under realistic environmental conditions. Inergen has a cup burner concentration of 29.1 vol% and a minimum design concentration of 34.9 vol% [32].

Because of the higher values, inergen requires more extensive storage than other suppressors, making it inappropriate for scarce locations like the maritime industry. Furthermore, inergen shows a slow distribution rate with higher required volumes, which is also a negative point.

2.10.3.2 Human safety

Including 8% CO₂ increases the human respiration rate and the heart rate to allow the human body to absorb oxygen at an oxygen level of 12%, making it suitable for occupied areas. However, there will be instances where the fraction of CO₂ level will be more than 10%, such as in a fire caused by hydrocarbons. Exposure to an environment with such a CO₂ level can lead to sudden unconsciousness, coma, and death. Therefore, it is recommended that personal protective equipment be used as much as possible. [32] Just like CO₂, N₂ and Ar in inergen contribute to reducing the O₂ levels in the environment. When more than 84% of N₂ and 33% of Ar are in an air mixture, they cause asphyxiation, which is O₂ deprivation. However, since inergen has lower concentrations of N₂ and Ar, there will not be an adverse effect on personnel by N₂ and Ar [33] [34].

The no observable adverse effects level (NOAEL) and lowest observable adverse effects level (LOAEL) are mainly defined as halogenic agents on cardiac sensitisation, described as the increased sensitivity of the heart to adrenaline. If the heart is made more sensitive to adrenaline, it can result in irregular heartbeat and possible heart failure. However, for inergen, the first adverse effect observed from the body because of the hypoxic environment is reduced oxygen supply to the brain, even though some of it is compensated by the high heart rate created by carbon dioxide.

For inergen, NOAEL is 52 vol% inergen, with at least 10% oxygen and around 5% CO₂. Medical studies have explained that the subjects showed normal intellectual functions with the mentioned combination, but without the carbon dioxide, the subjects exhibited confusion and loss of mental responses. The LOAEL level for inergen is 62%, with an atmospheric oxygen level of 8 % and a carbon dioxide level of 5-6%. A situation like this will have an increased level of hypoxia relative to the NOAEL level, although subjects will be able to escape the area without failing mental function [35].

The NOAEL and LOAEL for inergen are significantly higher than most fire suppressors, making it a strong candidate to apply to occupied areas.

2.10.3.3 Environmental impact

As inergen consists of atmospheric gases, it does not have the ozone depleting potential (ODP) and global warming potential (GWP). Inergen does not produce any products that are not environmentally friendly and products that are difficult to handle [32]. Therefore, inergen can be considered an environmentally friendly component compared to most other fire suppressors.

2.10.3.4 Applications of inergen

Burch et al. [32] did a study using a cumulative weightage system considering factors related to fire suppression to find a better replacement for halon 1301 suppressant, and they recommended inergen to be an effective fire suppression in occupied areas mainly because of its non-toxicity. Furthermore, since inergen does not have corrosive properties, it does not cause any damage to assets and properties and can be used with spots where sensitive items are placed.

Considering the properties inergen process, it can be used in areas like computer rooms, medical facilities, art galleries, machinery spaces, offshore facilities, and museums where occupancy can be expected. In contrast, sensitive assets and properties are placed.

2.11 Related work done

Jo and Crowl [36] have conducted experiments on hydrogen combustion in a 20-l spherical vessel to present explosion characteristics such as maximum explosion pressure and deflagration index. Their findings on the maximum explosion pressures indicated that the worst-case accidents for hydrogen-air mixtures in a confined volume might occur when the hydrogen concentration is at 29.5% - 40% on the more affluent side of the fuel, as shown in Figure 2.12. Furthermore, the study has proposed equations and methods for estimating the burning parameter and deflagration index. Shin [37] also studied hydrogen combustion with an ammonia mixture, and he obtained the maximum explosion pressure at around 800 kPa abs with a maximum pressure rise rate of around 270 [Mpa/s], as shown in Figure 2.13.

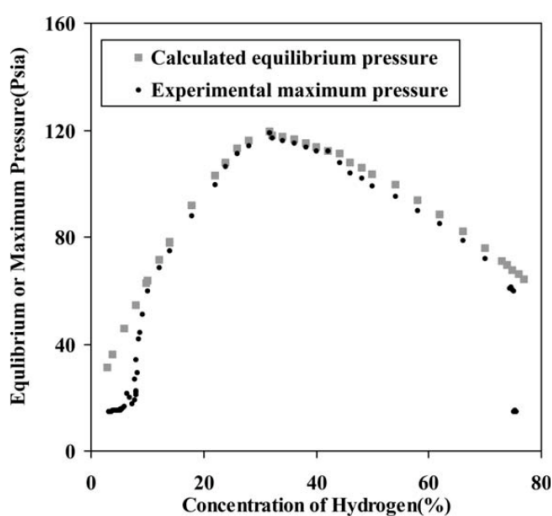


Figure 2.12: Maximum explosion pressure and equilibrium pressure of hydrogen-air mixture [36]

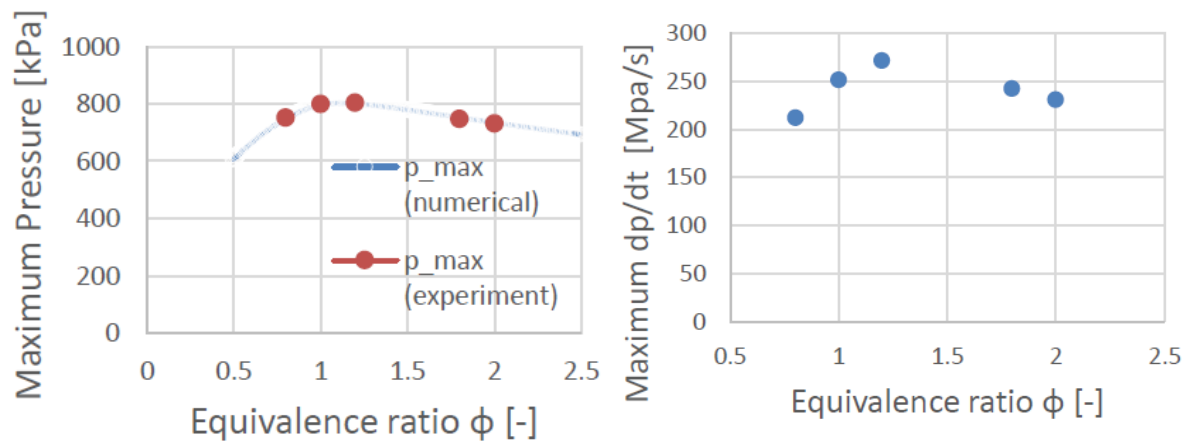


Figure 2.13: Experimental and computational result of H₂-air mixture explosion pressure (left) and experimental results of H₂-air maximum dp/dt values (right) at 100 kPa and 300 K [37]

Chen et al. [38], Zhao et al. [28] and Chen et al. [38] studied how adding nitrogen to flammable hydrocarbons will affect their flammability and found out the LFL of the fuel-air mixtures has little effect by adding the inert as expected from the theoretical study as shown in Figure 2.14. According to the calculations done by Chen et al., it was found that the inert abilities of CO₂ are stronger than nitrogen and helium.

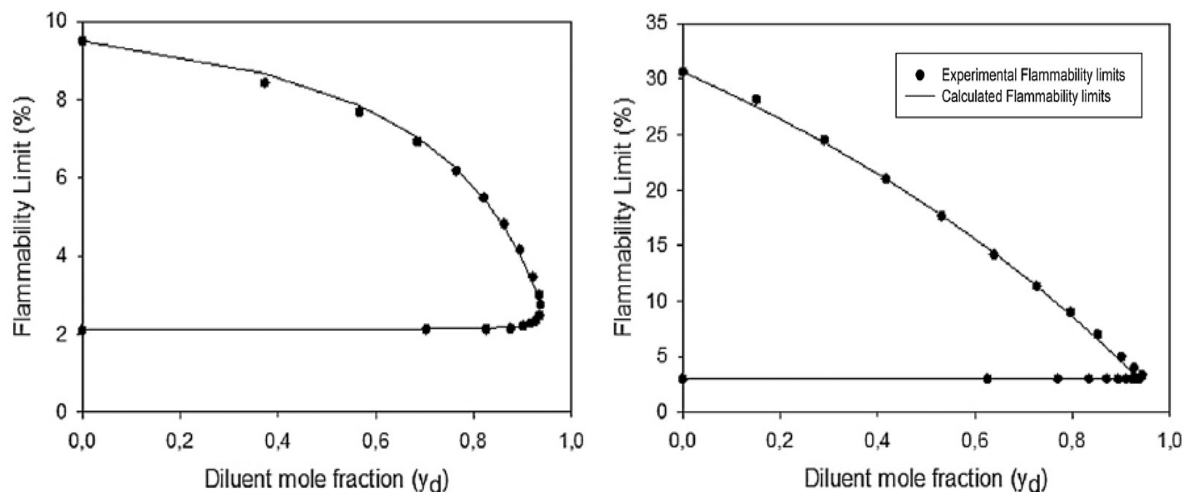


Figure 2.14: Comparison of experimental and calculated flammability limits for propane-N₂-air mixtures (left) and ethylene-N₂-air mixtures (right) at 25 °C and 1 atm.

Wang et al. [39] investigated hydrogen combustion with air when it is diluted with inert gases Ar, N₂ and CO₂ at room temperature and sub-atmospheric pressures. The study found out the maximum explosion pressure, maximum pressure rise rate, and deflagration index mainly depend on the initial pressure, the diluent type, and its fraction, as shown in Figures 2.15 and 2.16. Their study showed that 30% of CO₂ reduces the adiabatic temperature of the hydrogen flame to around 1900 K, while the same amount of N₂ and Ar reduces it to around 2300 K and 2500. In contrast, the hydrogen adiabatic air with no dilution was around 2700 K. The work also studied the linear correlations between normalised maximum explosion pressure and the diluent fraction.

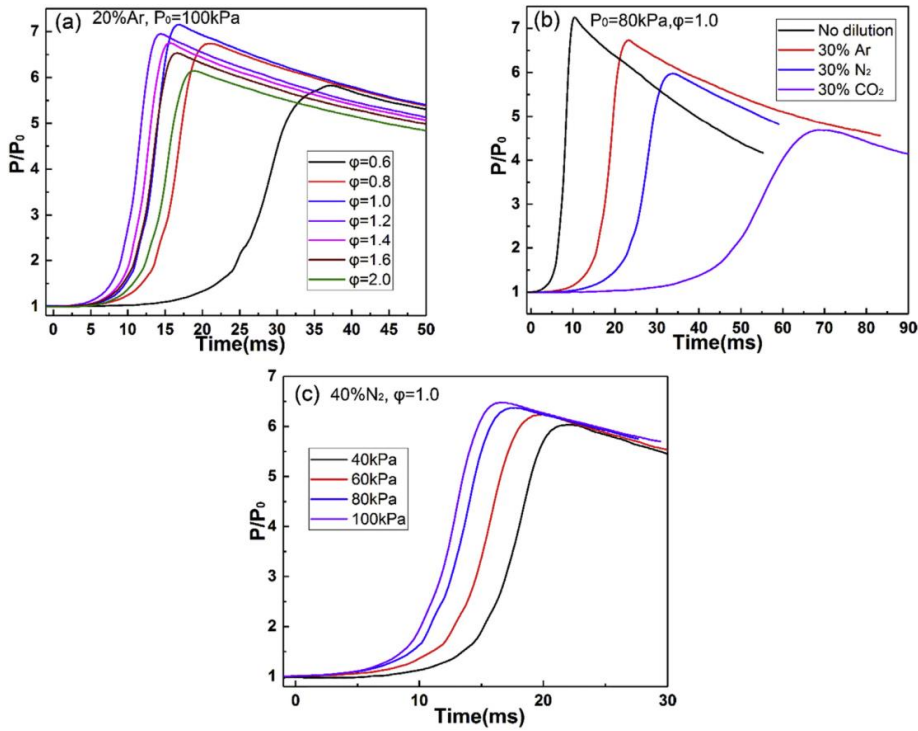


Figure 2.15: Hydrogen-air explosion pressure variations at various (a) equivalence ratios, (b) inert gases and (c) initial pressures [39].

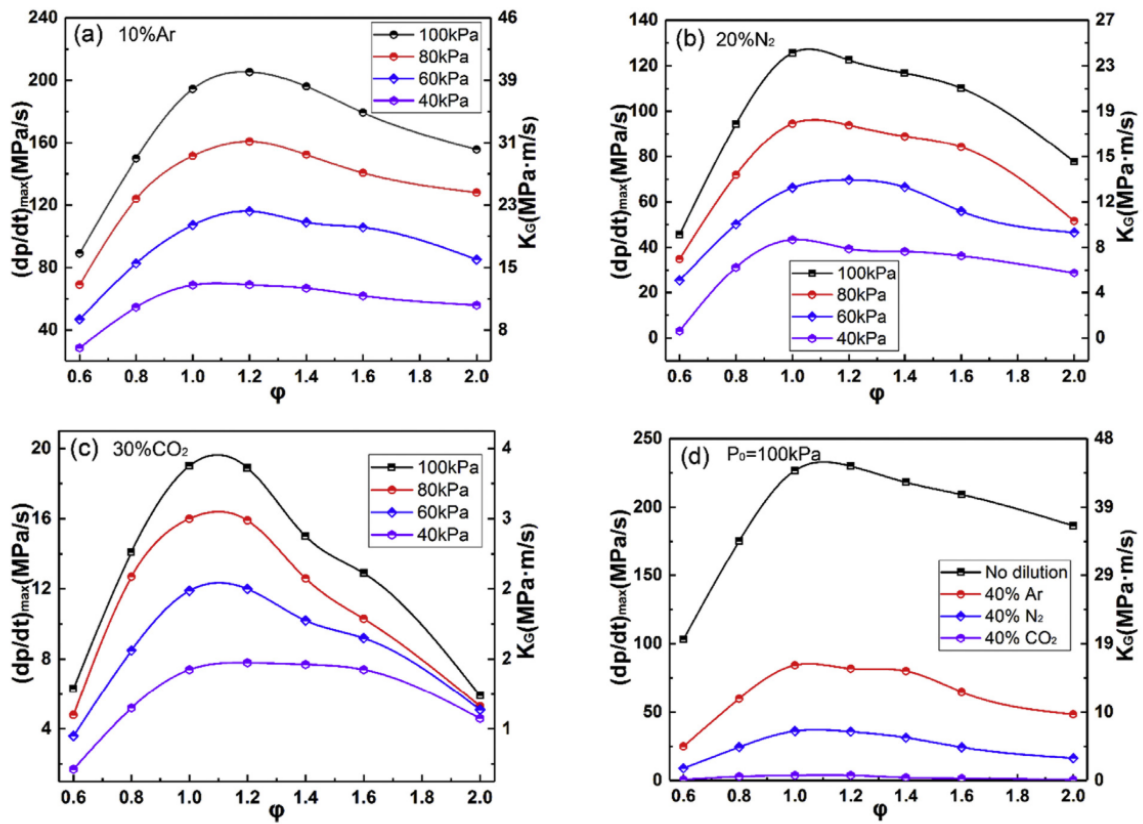


Figure 2.16: Maximum pressure rise rate and deflagration index with various inert dilutions [39].

Weiqiang et al. [40] ran experiments to study the inhibitory effects of inert gases, mainly N_2 and CO_2 , on suppressing the fires caused by the thermal runaway of lithium-ion batteries. Their study showed that nitrogen and carbon dioxide reduce the combustion temperature with their cooling effect and then the explosion intensities, as shown in Figure 2.17. As per their experiments, they observed that CO_2 showed better anti-explosion effects than N_2 , but neither of the inert gases could altogether terminate the combustion, and their batteries were reignited after the fire was extinguished. They also found that both the inert gases significantly affect batteries with a higher state of charge (SOC).

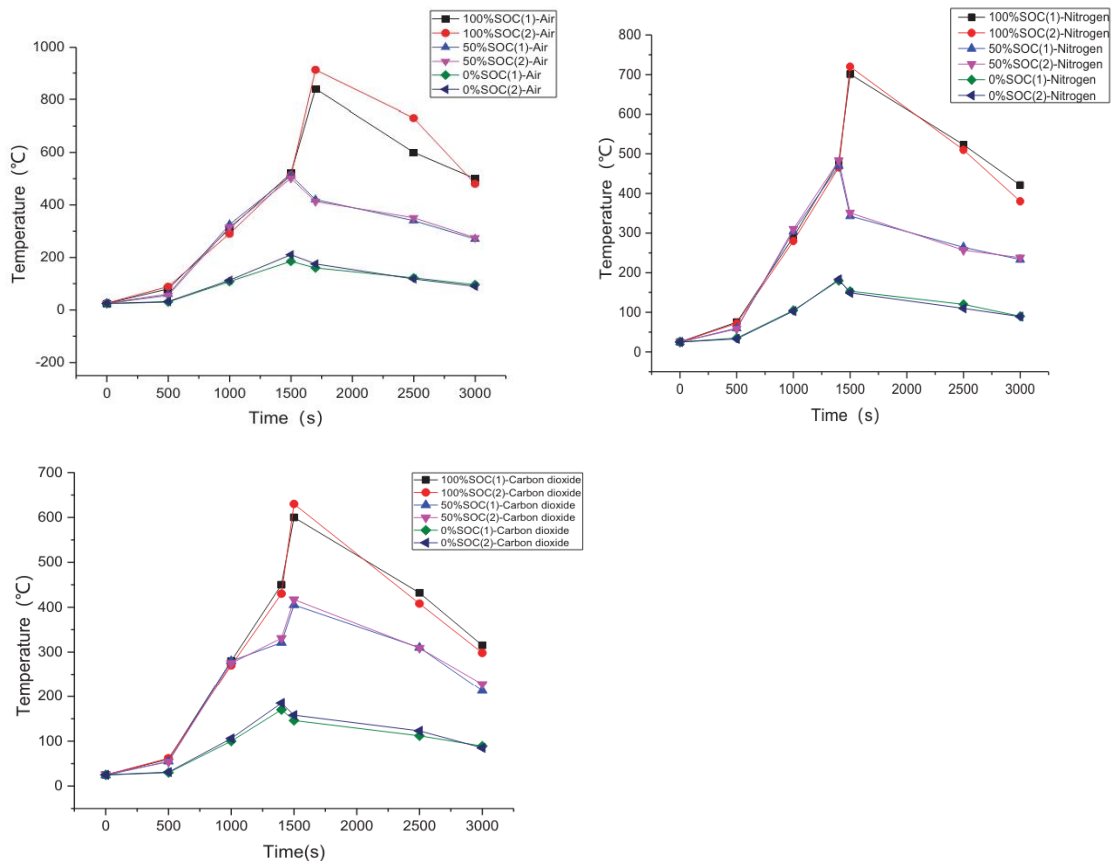


Figure 2.17: Lithium-ion battery combustion temperature change in air (upper left), N_2 (upper right) and CO_2 (lower) [40].

Saito et al. [41] developed an explicit relation for inert gas extinguishing concentrations considering their heat capacities and fuel properties. In this work, they considered 100% Ar, IG- 55 (50% Ar, 50% N_2), inergen and IG – 100 (100% N_2), CO_2 and some other inert gas mixtures. As shown in Figure 2.18, their work showed considerably better results for flammability limit variation with the added inergen and argonite with methane and propane. According to their findings, inergen has a low minimum inerting concentration (MIC) value of around 45% compared to 48% of argonite for methane.

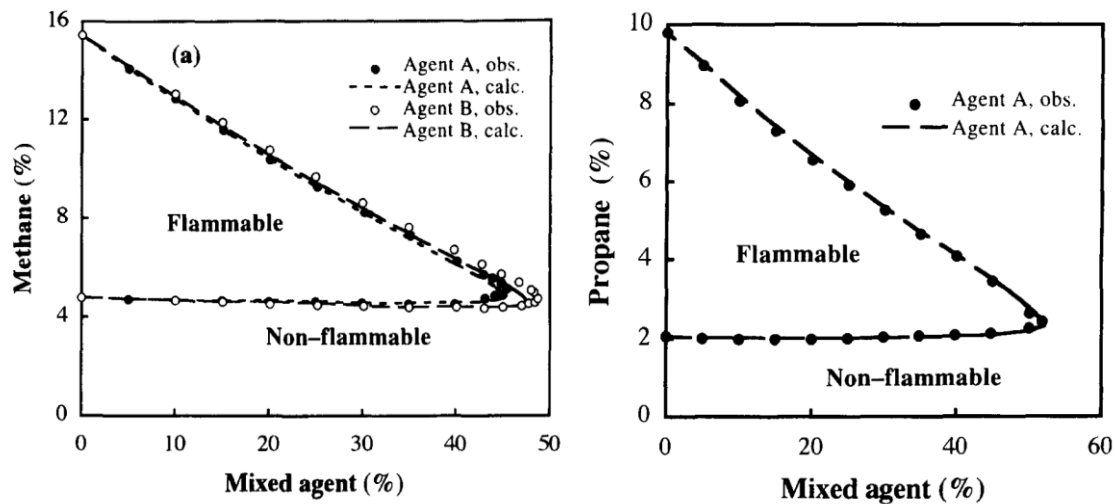


Figure 2.18: Observed (points) and calculated flammability limits (dashed lines) of methane-air (left) and propane-air (right) mixture with Agent A – Inergen and Agent B – Argonite [41].

Henriksen et al. [13] investigated the explosion characteristics of vented gases from LIBs. During thermal abuse testing, they collected a list of normalised gas compositions vented from the batteries. They proposed three battery gas compositions covering the upper and lower ranges of the LBV and a simplified gas to carry experiments in a 20-L explosion sphere. The explosion pressure, maximum explosion pressure rise rate, and the LBV values at 100 kPa and 300 K presented from their experiments are mentioned in Table 2.4. Battery gas with higher carbon dioxide exhibited lower maximum explosion pressures, while the battery gas with more H_2 and CO in the mixture showed higher maximum explosion pressures. This study also confirmed explosion property reduction due to an inert in a flammable mixture, in this case, battery gases.

Table 2.4: Laminar burning velocity, maximum explosion pressure and maximum rate of explosion pressure for the proposed battery gas compositions at 300 K and 100 kPa absolute [13]

Parameter	High LBV Li-ion gas	Low LBV Li-ion gas	Generic Li-ion gas
Laminar burning velocity (S_L) [mms^{-1}]	935	351	479
Maximum explosion pressure ($P_{ex})_{max}$ [MPa]	0.78	0.71	0.74
Maximum rate of explosion pressure rise $(dp/dt)_{ex}$ [$MPas^{-1}$]	81.68	22.59	32.89

3 Methodology

This chapter outlines the experimental configurations and computational resources utilised in the study. It is divided into two parts: the initial section discusses the setup of the 20-litre explosion sphere bomb and the procedure for conducting experiments. In contrast, the later delves part discusses the numerical techniques employed in Cantera.

3.1 Experimental setup

Details for the experimental apparatus mentioned below are the same information as the work done by Henriksen et al. [13] and shin [37] since they used the same experiment apparatus with a camera system to conduct their investigations.

Figure 3.1 exhibits the 20.4 dm³ sphere bomb apparatus setup used for the experiments. It consists of a steel sphere with insulation and a heating jacket to control the sphere temperature. Two filling ports were used to input inergen, and one port was divided into two lines so that port was used to input fuel and air. The port with air and fuel was purged carefully before adding one type of gas. An internal stirrer was used to mix the flammable mixture in the sphere to ensure a homogenous mixture was achieved before the explosion.

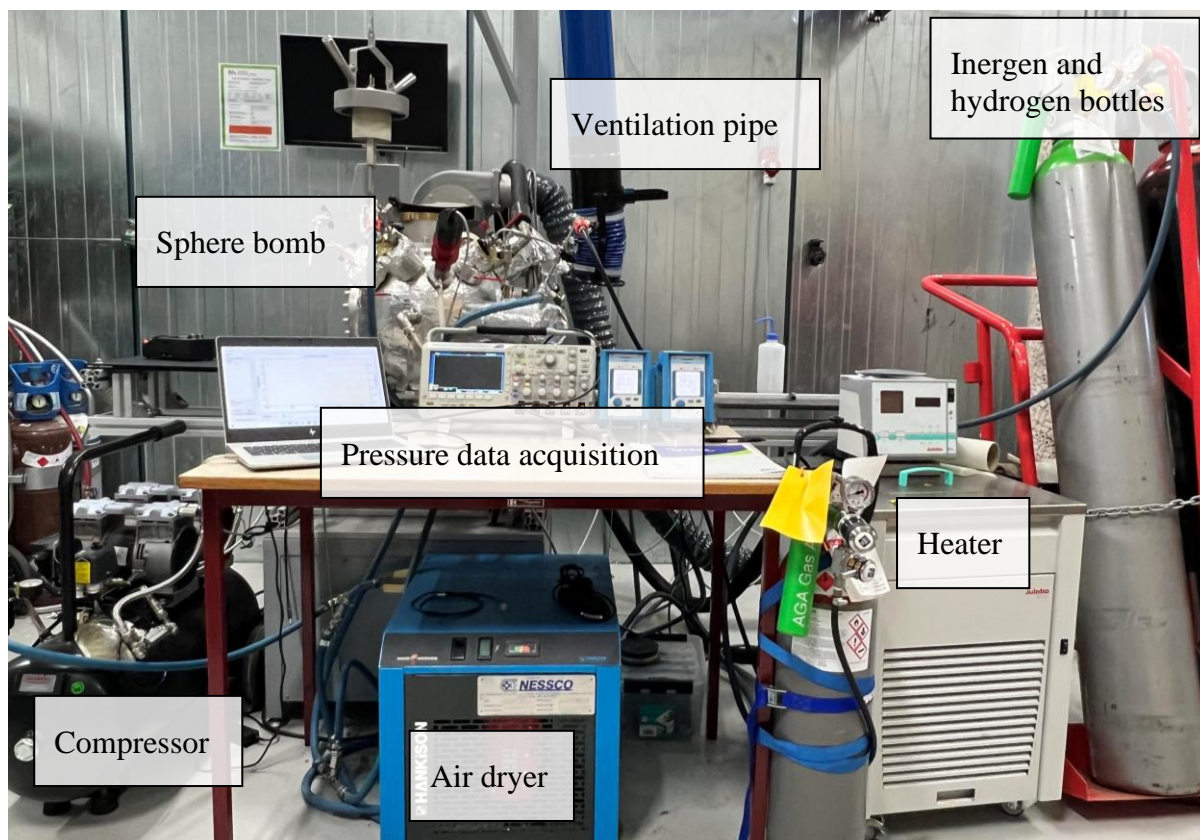


Figure 3.1: Sphere bomb used in the experiment.

An ignition coil with an inductance of 8.0 mH charged with 12 -15V was used to generate sparks. Two metal rods with a diameter of 1 mm were connected to the ignition coil, and the spark gap between two metal wires was from 1mm to 4 mm. The energy released for each spark is about 100 mJ, with a voltage of 30 kV.

Three pressure sensors were used to get pressure measurements: one was used to measure the internal pressure of the sphere while it was filling; namely, Keller PAA-33X, and two Kistler 601CAA pressure sensors were used to measure explosion pressures. The apparatus could measure flame velocity using high-speed cameras, which was not used in this experiment. Figure 3.2 shows a schematic diagram of the experimental setup.

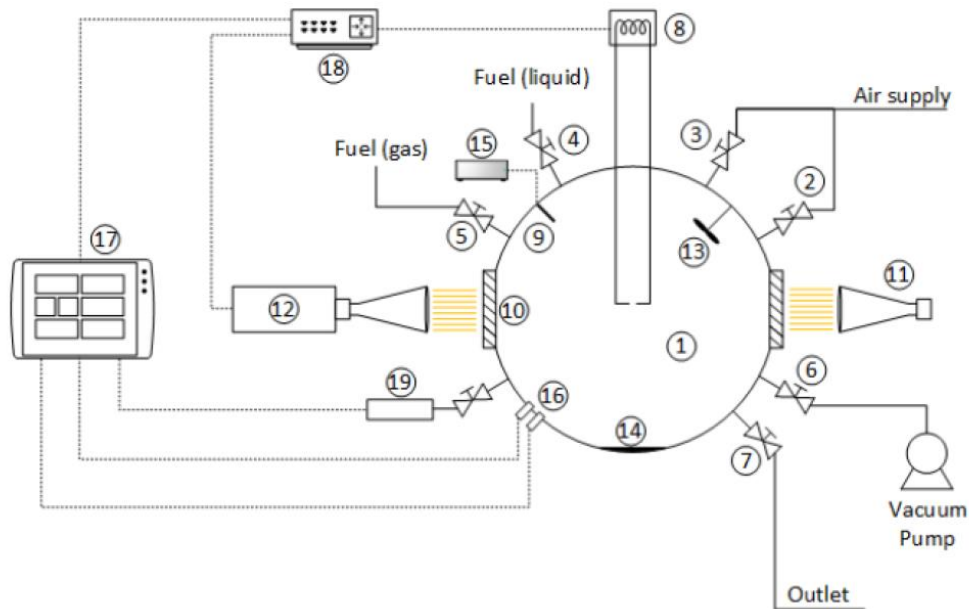


Figure 3.2: Schematic diagram of experimental setup [11]. 1: explosion chamber; 2: oxidiser inlet; 3: flush inlet; 4: fuel (liquid) injection port; 5: fuel (gas) inlet; 6: vacuum port; 7: gas outlet; 8: ignition system; 9: thermocouple; 10: glass windows (100 mm); 11: LED light source; 12: high-speed camera; 13: stirrer; 14: heating plate; 15: ambient temperature display; 16: dual explosion pressure sensors; 17: data acquisition system; 18: control/trigger unit and 19: ambient pressure sensor

3.1.1 Materials used

Three types of flammable gases were used to study the effect on inergen, including hydrogen and two types of battery gases used by Henriksen et al. [13], which cover higher LBV end of battery-vented gas and an averaged battery-vented gas. Compounds used for the experiments and their compositions are mentioned in table 3.1 below,

Table 3.1 Chemicals used in the experiment.

Compound	H ₂ [%]	O ₂ [%]	N ₂ [%]	CO [%]	CO ₂ [%]	CH ₄ [%]	C ₂ H ₄ [%]	Ar [%]
Air	-	21	79	-	-	-	-	-
Hydrogen	100	-	-	-	-	-	-	-
Inergen	-	-	-	-	8	-	-	40
High LBV Li-ion gas	42.8	-	-	37.1	10	7.1	3	-
Generic Li-ion gas	34.9	-	-	25	20.1	15	5	-

As mentioned in Table 3.2, with the three fuel types used in the experiment, 3 sample types were used for hydrogen, and two were used for battery gases.

Table 3.2: Mixture types used in the experiments.

Fuel type	Mixture type 1	Mixture type 2	Mixture type 3
Hydrogen	Mixed with 100% air	Mixed with 50% air and 50% inergen	Mixed with 25% air and 75% inergen
High LBV Li-ion gas	Mixed with 50% air and 50% inergen	Mixed with 25% air and 75% inergen	-
Generic Li-ion gas	Mixed with 50% air and 50% inergen	Mixed with 25% air and 75% inergen	-

3.1.2 Procedure of experiment

Before every single experiment, the sphere was purged with oil and compressed air for more than 5 minutes to remove any unwanted components in the sphere, such as soot and water produced by the combustion process. After purging, the ignition coil was set, and the sphere was sealed to fill the required mixture. Fuel, inert and air were filled into the sphere until it reached 100 kPa. Then, the mixture was stirred for around 5 minutes and rested for another 3 minutes to achieve a homogenous and quiescent mixture. Then, after recording the final conditions, the mixture was ignited. After the ignition spark, it was checked whether combustion occurred or not. Then, the pressure data was saved to the computer. A safety checklist was thoroughly followed to ensure smooth flow of the investigation as mentioned in Appendix C.

A total of 82 shots were taken on the explosion sphere with different mixture compositions, which could be found in Annex B. Eight of the 82 explosions were done to get used to the explosion sphere. Fifteen experiments were not considered in Chapter 4 since there were either dry runs with air, the flammable mixture ended up in a significantly higher pressure than 1 atm, or the pressure was not constant when all the valves were closed due to boiling of the residual water droplets. The sphere was purged with filtered air while the sphere was heated up to 45 °C for around 30 to 60 minutes to overcome this issue.

3.1.3 Maximum explosion pressure and maximum rate of explosion pressure rise

Materials used for measuring explosion pressure are consistent with those described in Chapter 3.1. A 20-litre explosion sphere is fitted with dual pressure sensors. The explosion pressure measurement is post-filtered to reduce noise. All experiments have identical smoothing-filter parameters at 999 data points and a second-order polynomial fit. The average pressure value obtained from the dual sensors represents the mean maximum explosion pressure [37].

3.1.4 Maximum rate of explosion pressure rise

Maximum rate of explosion pressure rise $(dP/dT)_{max}$ is measured based on data from two pressure sensors. Utilising Python, each most significant gradient with positive values of filtered pressure data is calculated, and the average value is used to calculate the mean maximum rate of the rise in explosion pressure. Figure 3.4 shows a sample of the plot.

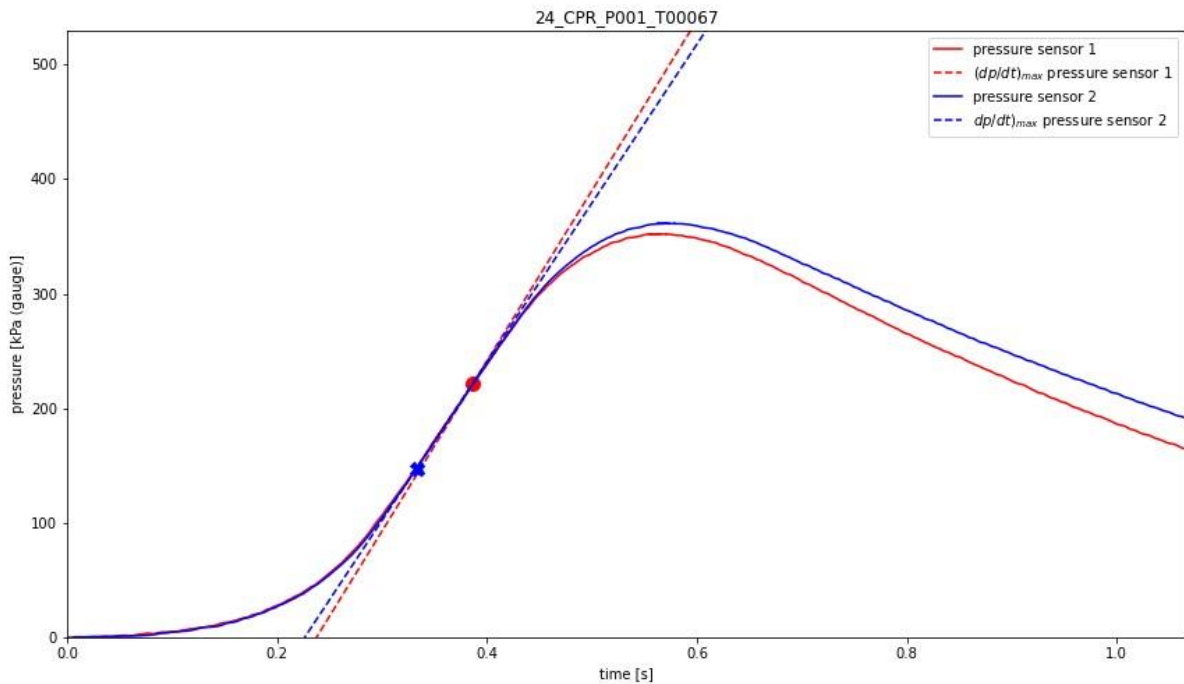


Figure 3.3: Processed result of a maximum rate of explosion pressure rise using two pressure sensors.

3.2 Cantera Numerical calculation

3.2.1 Maximum explosion pressure

The 'equilibrate' solver of Cantera is employed, which calculates composition with minimum Gibbs free energy, maintaining constant volume and internal energy state to compute the explosion pressure and rate of explosion pressure rise.

3.2.2 Flammability limit approximation

A simple model was created using the built constant enthalpy equilibrate function in Cantera, which uses the thermodynamic parameters of the species to participate in the reaction to find an approximation of the flammability limits of fuel with added inergen. UFL and LFL were approximated by giving minimum adiabatic flame temperature at LFL and UFL using the literature values. The adiabatic flame temperature for hydrogen was 867 K at its LFL while 1135 at the UFL. However, adiabatic flame temperatures could not be found at their flammability limits for the chosen battery gases. Therefore, they were approximated, considering their compositions and the literature they found [42]. Since accurate adiabatic temperatures were not found for battery gases, the approximations done to battery gases were not added to the report but annexed in Appendix D.

Figure 3.4 explains how the approximated flammability limits were obtained for the fuel used in this experiment. The simulation started with 0 % inergen dilution, and the inergen was added in a loop until it reached the adiabatic flame temperature given. The inergen amount required and the fuel concentration are recorded as the flammability limit. The Python code ran using Cantera can be found in the Appendix F.

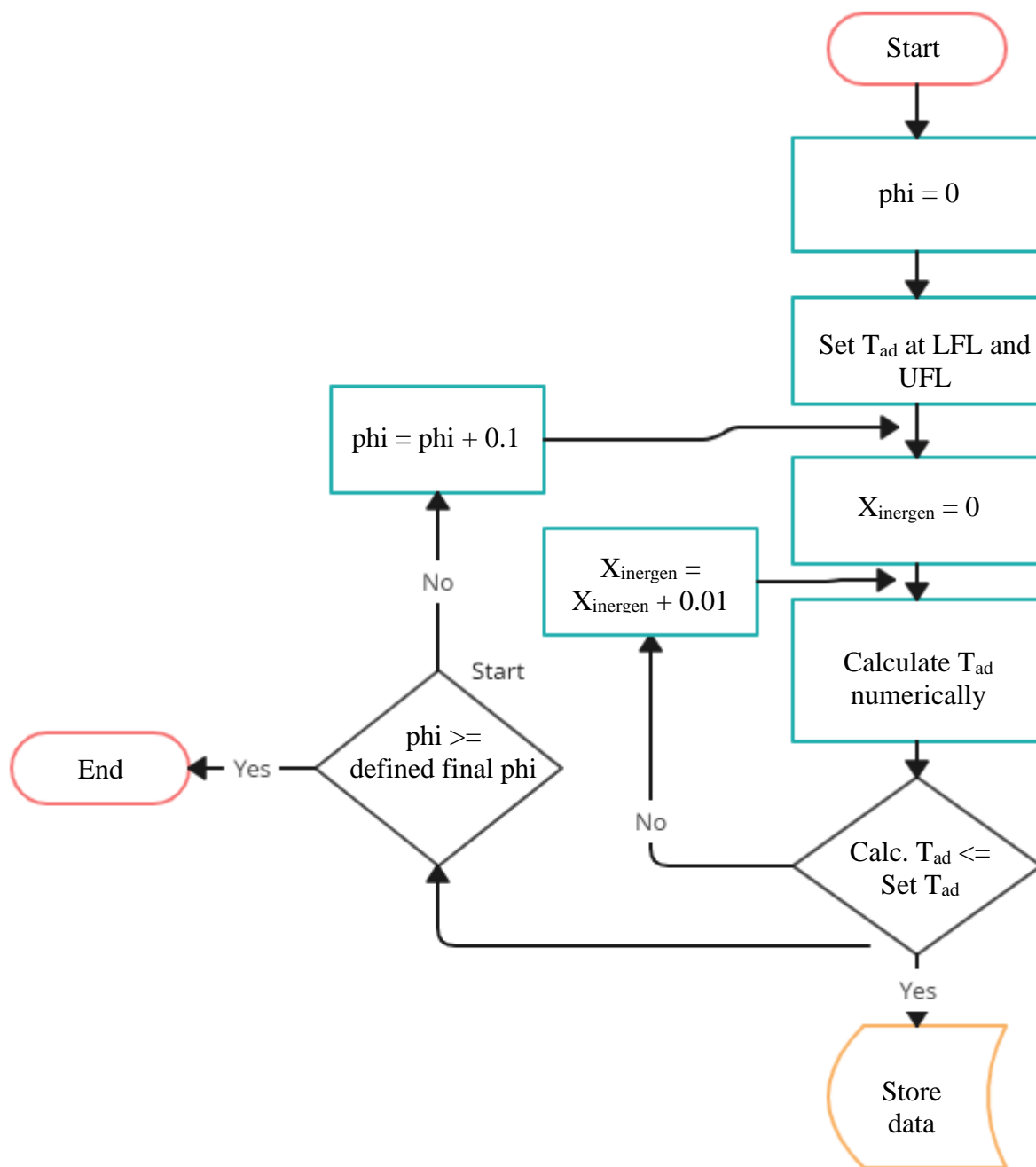


Figure 3.4: Model simulation algorithm to find flammability limits.

4 Results

This chapter consists of the results of experiments on maximum explosion pressure, maximum pressure rise, deflagration index, and a flammability limit analysis using a numerical approximation. Chapter 4.1 reports the maximum explosion pressure data obtained from the experiments with the numerical explosion pressures. Chapter 4.2 presents post-processed maximum explosion rise and deflagration index values. In the last chapter, how flammability limits are affected by adding inergen to a flammable mixture was compared using a simple numerical approximation and the experimental results.

4.1 Maximum explosion pressure

4.1.1 Hydrogen combustion with inergen

As shown in Figure 4.1, three types of experiments were carried out to observe how inergen affects the maximum explosion pressure of hydrogen with different inergen compositions in the flammable mixture. As expected, the observed explosion pressures were lesser when more energy was added to the flammable mixture. According to the results, hydrogen with 100% air obtained a maximum explosion pressure of 696.11 kPag at an equivalence ratio of 1.06. In comparison, hydrogen with 50% air and 50% inergen obtained 494.75 kPag pressure at an equivalence ratio of 1.21, closer to stoichiometric conditions. Hydrogen with 75% inergen and 25% air obtained the most negligible maximum explosion pressures, where at 1.25 equivalence ratio, it obtained a maximum pressure of 152.34 kPag.

Furthermore, the maximum explosion pressures were observed near the stoichiometric composition ratios for all three experiments. However, the smoothness of the simulation data is reduced with the inergen concentrations, and the experimental data also showed some discrepancies.

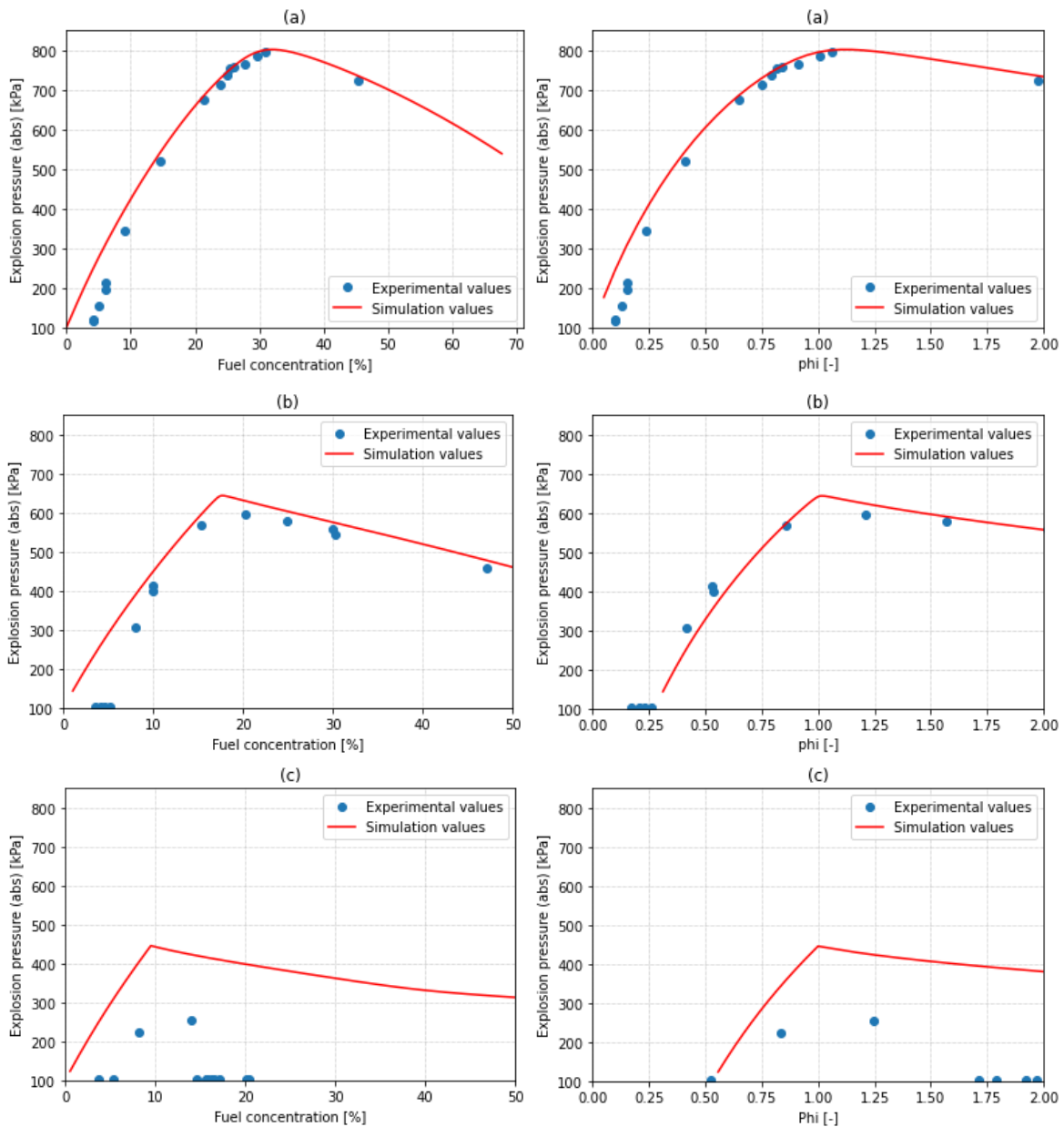


Figure 4.1: Comparison between experimental and computational results. Left: 'Fuel concentration vs. maximum explosion pressure' with different H₂/Air/Inergen ratios. Right: 'Fuel equivalence ratio vs. maximum explosion pressure' with different H₂/Air/Inergen ratios at 300K and 1 atm. (a) H₂ with 100% air, (b) H₂ with inergen 50% + air 50% mixture, (c) H₂ with inergen 75 % + air 25% mixture

4.1.2 Battery gas combustion with inergen

As mentioned in Chapter 3.1.1, High LBV and a generic battery gas were used in the experiment to observe how the maximum explosion pressure behaves with inergen. Figure 4.2 presents the maximum explosion pressures measured for each battery gas with the oxidiser with 50% and 75 % inergen concentration. The measured results were significantly lower than the simulation results. Furthermore, even with the near stoichiometric compositions, neither battery gas ignited with 75% inergen composition in the oxidiser.

High LBV battery gas with 50% inergen and 50% air obtained a maximum explosion pressure of 483.01 kPag at an equivalence ratio of 1.03, while the generic battery gas obtained 228.11 kPag at 0.81 equivalence ratio.

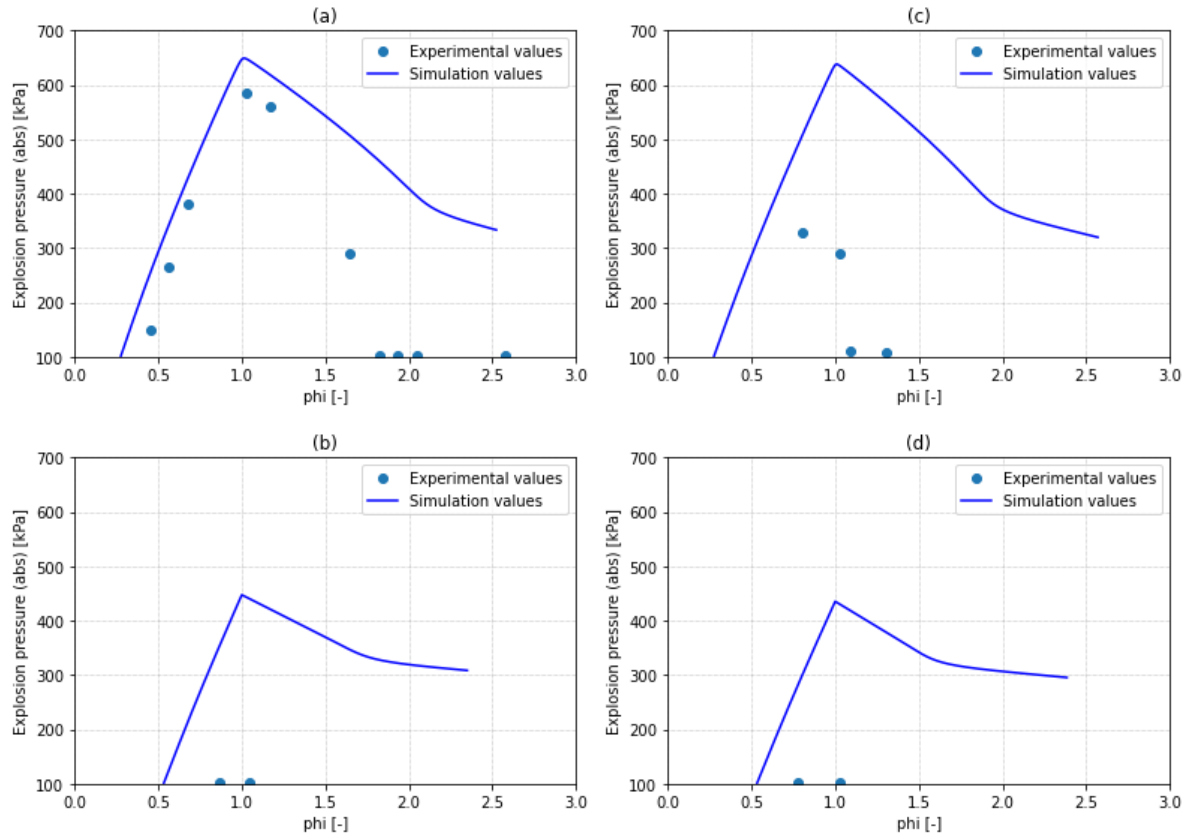


Figure 4.2: Comparison between experimental and computational results for battery gases. 'Fuel equivalence ratio vs maximum explosion pressure' with different Battery gas/Air/Inergen ratios at 300K and 1 atm. (a) High LBV battery gas with air mixed with 50% inergen, (b) High LBV battery gas with air mixed with 75% inergen, (c) Generic battery gas with air mixed with 50% inergen, (d) Generic battery gas with air mixed with 75% inergen

4.1.3 Maximum explosion pressure ratio $\left(\frac{P_{ex}}{P_o}\right)$

The maximum explosion pressure ratio can be calculated using the maximum and initial pressure of the flammable mixtures. Figure 4.3 shows how the peak explosion pressures vary with the hydrogen composition with the inergen inclusion. Hydrogen mixtures without inergen showed a maximum peak explosion ratio of 6.85 at an equivalence ratio of 1.06, near the stoichiometric levels. In contrast, mixtures with inergen showed a low peak explosion ratio proportional to the inergen added. In contrast, hydrogen with 50% air and 50% inergen showed an explosion ratio of 4.93 at an equivalence ratio of 1.21, the closest to the stoichiometry among the samples. As expected, 75% air and 25% inergen mixture obtained the least maximum explosion ratio of 1.49 at the equivalence ratio, which was 1.25.

As mentioned earlier, the battery vented gas mixtures with air 25% and inergen 75% did not burn. Therefore, peak explosion pressure ratios for the battery gases when mixed with only 50% inergen and 50% air are shown in Figure 4.4. High LBV battery gas obtained a higher peak explosion ratio of 4.76 near the stoichiometric levels, closer to the hydrogen mixture with

50% inergen and 50% air. Generic battery gas showed a closer peak explosion pressure ratio of 2.25 at an equivalence ratio of 0.81 to hydrogen with 25% air and 75% air mixture.

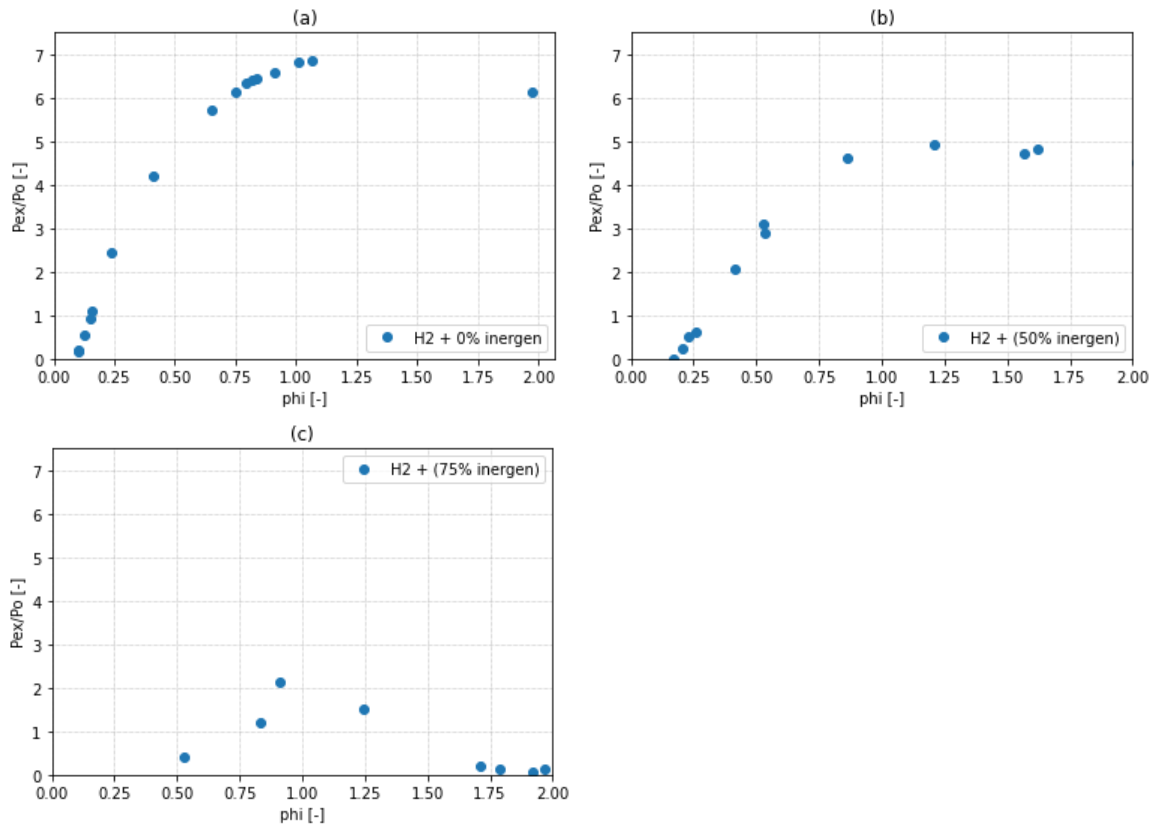


Figure 4.3: Experimental result of 'Equivalence ratio – Maximum explosion pressure ratio for different hydrogen mixtures at 300K and 1 atm. (a) H_2 with 100% air, (b) H_2 with inergen 50% + air 50% mixture, (c) H_2 with inergen 75 % + air 25% mixture.

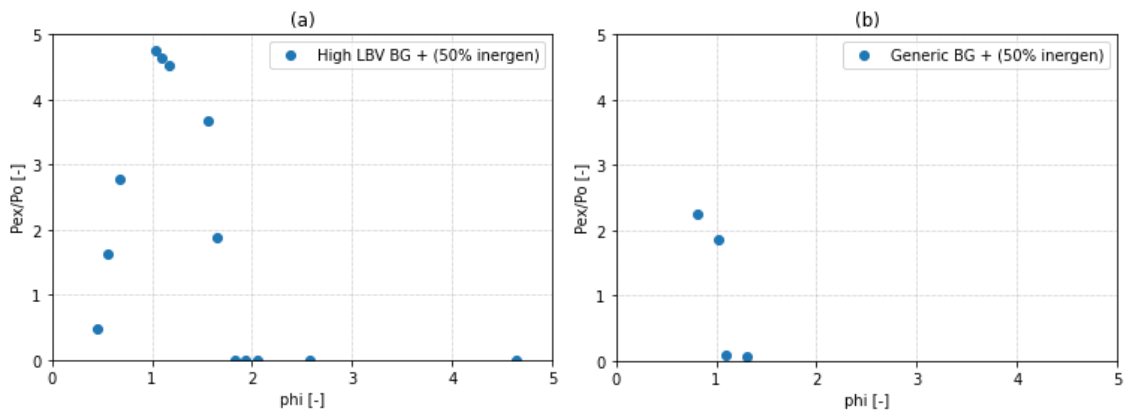


Figure 4.4: Experimental result of 'Equivalence ratio – Maximum explosion pressure ratio for different hydrogen mixtures at 300K and 1 atm. (a) High LBV battery gas with air mixed with 50% inergen, (b) High LBV battery gas with air mixed with 75% inergen

4.2 $(dp/dt)_{max}$ values and K_G values

4.2.1 Maximum rate of explosion pressure rise

Maximum rate of explosion pressure rise $(dp/dt)_{max}$ of the experiments were obtained using post-processing of explosion data. Figure 4.5 illustrates how the maximum rate of explosion rise varies in hydrogen-air mixtures with the inclusion of inergen. As expected, the pure hydrogen-air mixture performed a maximum explosion pressure rate of 289 MPa/s around its stoichiometry, but it significantly dropped with the inclusion of inergen, where hydrogen with 50% air and 50% inergen showed a maximum $(dp/dt)_{max}$ of 46.18 MPa/s at an equivalence ratio of 1.21, the closest to the equivalence ratio among the relevant samples. hydrogen mixture with 25% air/ 75% inergen as its oxidiser showed 0.58 MPa/s of $(dp/dt)_{max}$ near its stoichiometry, which is 0.84 of equivalence ratio, which can be easily observed in Figure 4.7.

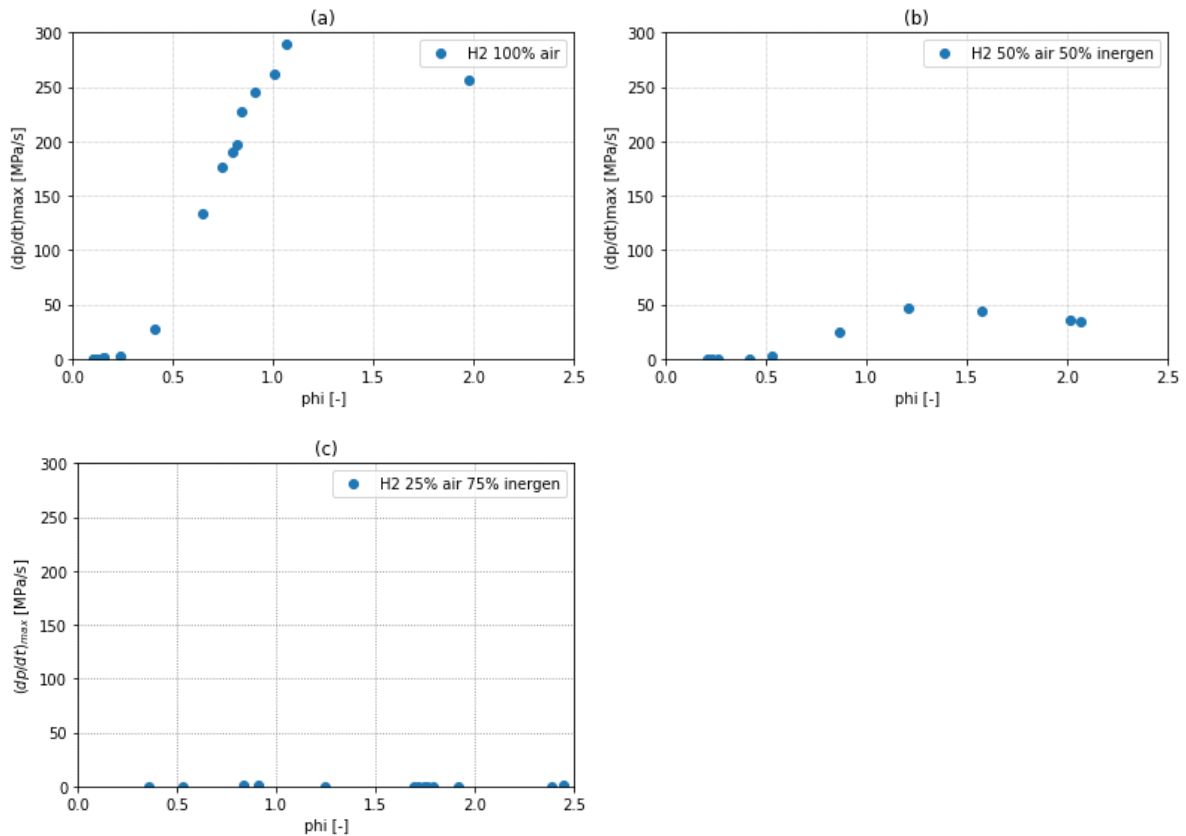


Figure 4.5: Experimental result of 'phi – Maximum rate of explosion pressure rise' with different H₂/air/inergen compositions at 300K and 1 atm. (a) H₂ + (100 % air), (b) H₂ + (50% air + 50% inergen) (c) H₂ + (25% air + 75% inergen).

Similarly, Figure 4.6 represents the $(dp/dt)_{max}$ values for the experiments with battery gases were mixed with a mixture of 50% air and 50% inergen. Since battery gases did not burn with 75% inergen and 25 % air mixture, they were not plotted for their explosion pressure rise data. Compared to hydrogen, battery gases showed shallow maximum pressure rise values when diluted with 50% inergen, where the high LBV gas obtained a $(dp/dt)_{max}$ of 6.04 MPa/s at its equivalence ratio of 1.03, while the generic gas recorded a 0.61 MPa/s pressure rise rate at 0.81 equivalence ratio.

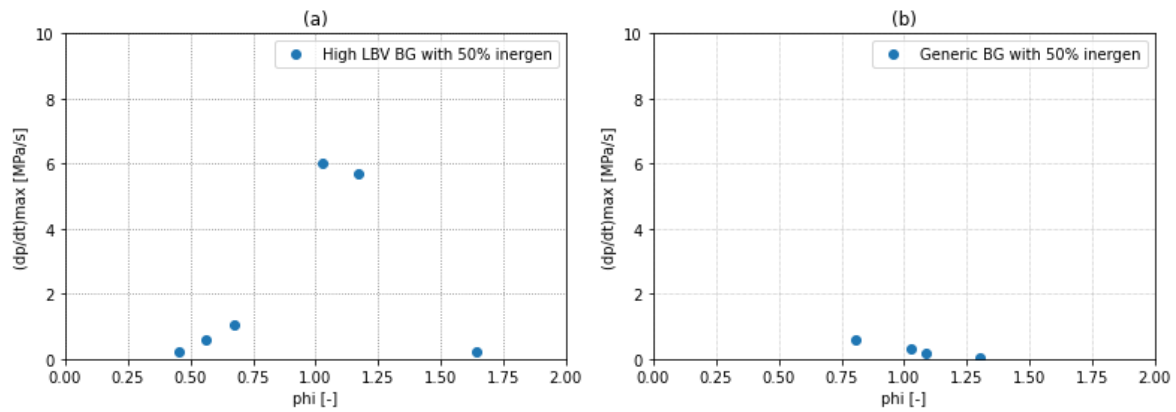


Figure 4.6: Experimental result of 'Equivalence ratio – Maximum rate of explosion pressure rise' with battery gases with air 50% and inergen 50% mixtures. (a) High LBV battery gas + (50% air + 50% inergen) (b) Generic battery gas + (50% air + 50% inergen).

Figure 4.7 illustrates all the logarithmic. $(dp/dt)_{max}$ gained from explosions with all different flammable mixtures with their equivalence ratios, which is more straightforward to observe where hydrogen mixtures have obtained higher $(dp/dt)_{max}$ values.

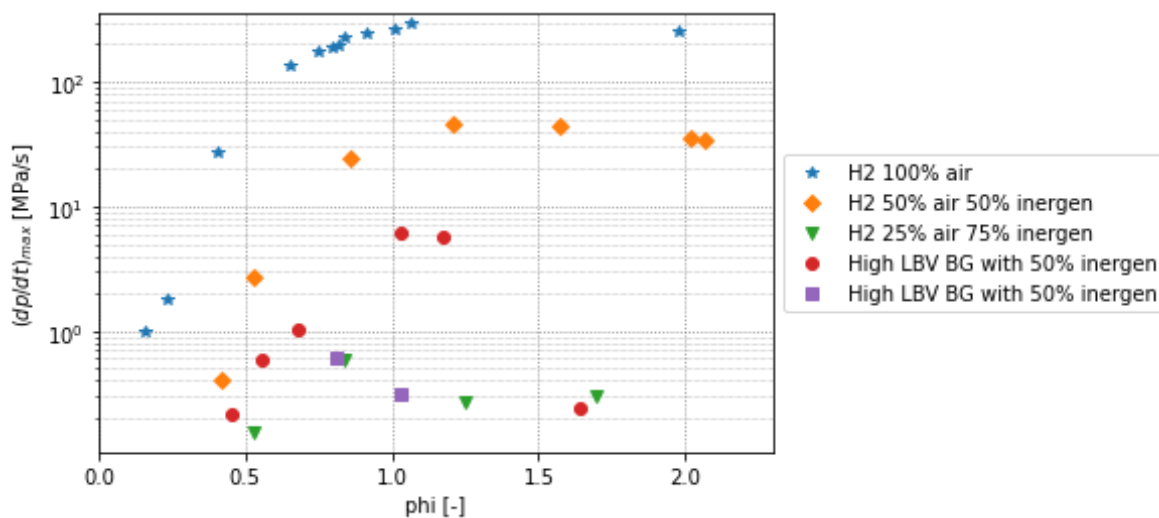


Figure 4.7: Experimental results of 'Equivalence ratio – Maximum rate of explosion pressure rise' with all the fuel mixture types.

4.2.2 Deflagration index (K_G) values

The processed deflagration index values for the burnt flammable mixtures are illustrated in Figure 4.8. Hydrogen mixtures with 100% air significantly gained a higher deflagration index of 791.66 bar.m/s at a 1.06 equivalence ratio which is higher than the value Crowl et al. [36] mentioned which is 659 bar.m/s. In comparison, hydrogen with 50% inergen and 50% air obtained 126.18 bar.m/s at a 1.21 equivalence ratio, and hydrogen with 75% inergen and 25% air gained a maximum deflagration index of 1.58 bar.m/s at the equivalence ratio of 0.84.

On the other hand, high LBV battery gas with 50% inergen and 50% air at an equivalence ratio of 1.03 gained a deflagration index of 16.49. In contrast, the generic battery gas with the same dilution gained 1.66 bar.m/s at 0.81 equivalence ratio.

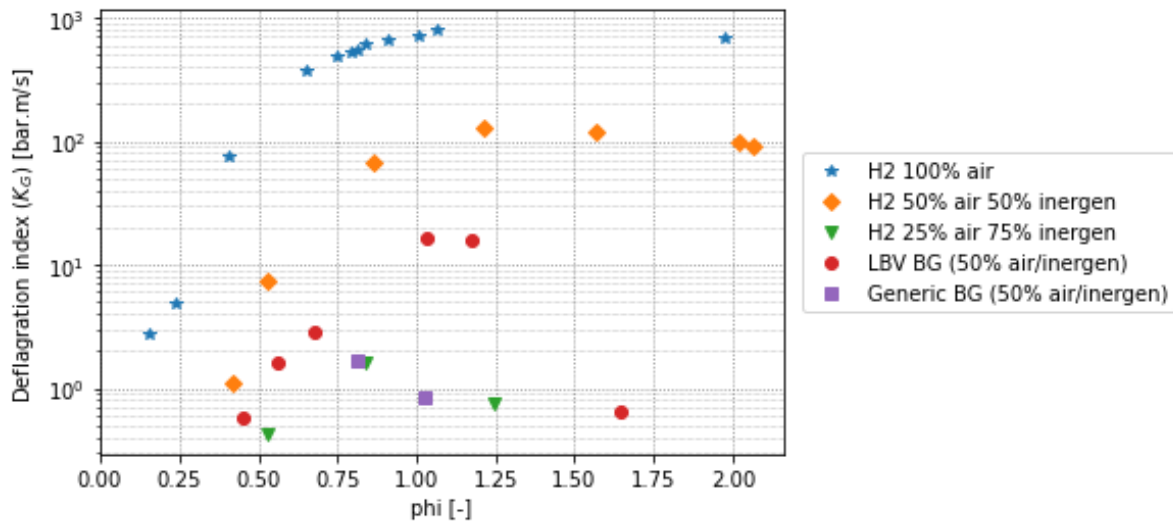


Figure 4.8: Experimental results of 'Equivalence ratio – Deflagration index' with all the burnt fuel mixture types.

4.3 Simple flammability limits analysis

As discussed in Chapter 3.2.2, a simple model was constructed using thermodynamic equilibrium using the adiabatic temperatures of fuels at the flammability limits. Then, this model was fitted with the experiments on where they stand in the model.

4.3.1 Hydrogen flammability

Hydrogen has an LFL of 4% and UFL of 75% in air. As shown in Figure 4.9, hydrogen shows 76% for UFL and 7% for LFL, which deviates from the actual values. However, this result was compared with the experimental results for a qualitative analysis. All the burnt samples are fit inside while the unburnt ones fit outside of the approximation, which can be used to confirm the experimental results.

In the simulated approximation, UFL varies in a straight line with the inert added, but in the actual scenario, it does not change in a straight line but in a curved line near the nose. However, the qualitative UFL of hydrogen reduces significantly with the dilution of inergen, while LFL does not change significantly, which agrees with the literature of Zhao [28] and Chen [38]. According to the approximation, the limiting oxygen concentration (LOC) or the minimum ignition concentration (MIC) is around 77% of the inergen in the mixture, which means that after 77% of the inergen in the mixture, there is no point in concentrating it more with inergen because the mixture will not be ignited because of lack of oxygen.

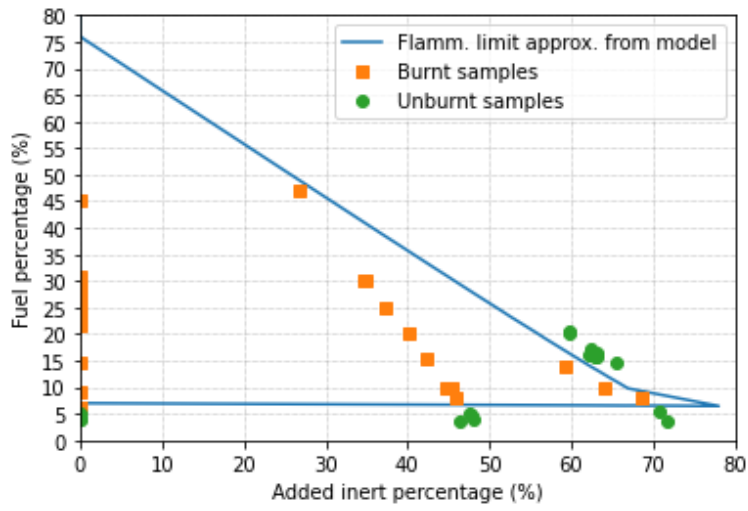


Figure 4.9: Numerical approximation for flammability variation for hydrogen with inergen added, with burnt and unburnt samples given.

5 Discussion

In this chapter, the results of the study will be analysed and discussed. Chapter 5.1 compares the experimental results with the literature found in this study and the computational results obtained from this study. Chapter 5.2 discussed the maximum explosion pressures obtained during the experiments and why the different values were obtained for various mixtures. Chapter 5.3 explained why the maximum rate of explosion pressure rise and deflagration index values varied with different mixtures. Chapter 5.4 showed how inergen affects the oxygen concentration in a flammable mixture to suppress a fire. Finally, Chapter 5.5 suggested the approximated flammability limits on the recommended inergen levels by Burch et al. [32] in their study.

5.1 Validation of experimental results

5.1.1 Comparing experimental values with the literature

A comparison between the found literature values and the maximum explosion values from the experiments was made to ensure that the equipment gives acceptable results. Figure 5.1 compares the maximum explosion pressures of pure hydrogen combustion with air between this experiment and a study by Jo and Crowl [36]. The comparison shows that the experimental values of this study agree with the literature. Furthermore, Figure 5.1 (a) ensures that the numerical values verify the experimental data.

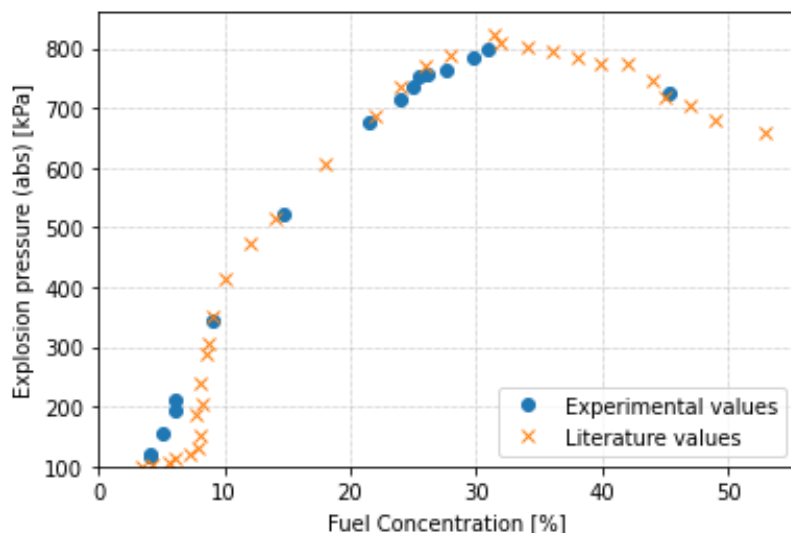


Figure 5.1: Comparison between hydrogen maximum explosion pressure experimental results vs. the results found from literature at 300 K and 1 atm [36].

Since the studies related to hydrogen combustion with inergen were not found, a simple numerical analysis was done considering the thermodynamic properties of the mixtures using Cantera with constant enthalpy calculations, as described in Chapter 3.2.2. This model was compared, as shown in Figure 5.2, with the data from the study by Saito et al. [41], where inergen was used as an inert with methane and propane combustion.

The developed model seemed to agree with the study done by Saito but with some deviations. Furthermore, the literature has shown a lower MIC than the approximation for both fuels. This

can happen due to several factors. The approximation done in this study is not an actual combustion simulation but a thermodynamic approximation without any heat loss, intermediate components, or reactions. Nevertheless, this work was done to understand how inergen affects flammability and what flammability levels can be achieved by introducing inergen into a mixture.

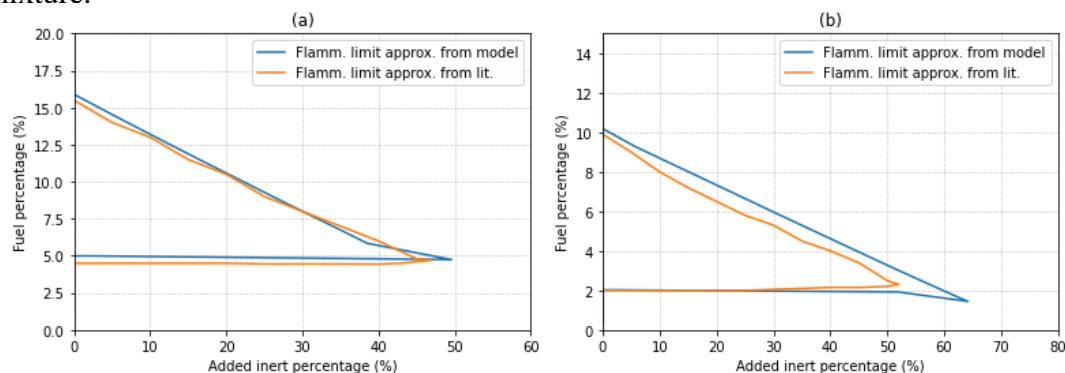


Figure 5.2: Flammability variation with added inergen between literature and the present work at 300 K and 1 atm for (a) methane and (b) propane [41].

5.1.2 Comparing experimental values with the simulated values

Among the experiments done, the experiments without inergen agreed well with the computational results. However, with the inclusion of inergen, the results showed deviations from the simulated values. Most of those results deviated lower than the simulated values.

Computational simulations using Cantera in Python are done in adiabatic conditions without any heat loss to the outside. However, in the actual scenario, there is always heat loss, like radiation, during the experiments. With the slow flame propagation, it takes a much longer time for the reaction to be completed. Therefore, the more time the reaction happens, the more heat will be lost. This is the main reason the experiments with inergen showed variations in the computed values.

5.2 Maximum explosion pressure

This work and the studies by Jo and Crowl [36] and Shin [37] presented a maximum explosion pressure of around 800 kPa for H₂/air mixtures at stoichiometry. Nevertheless, as expected, hydrogen maximum explosion pressure reduced with the introduction of inergen, 494 kPag for H₂ with 50% air and 50% inergen mixture and 152.34 kPag with 25% air and 75% inergen at near stoichiometric conditions. This happens mainly due to heat loss during the flame propagation, with the added inert. Inergen does not participate in the reaction but absorbs the heat generated by the combustion reaction, leading to low heat to continue the flame. Furthermore, added inergen reduces the air concentration of the mixture, hence the oxygen levels. Therefore, inergen suffocates the mixture by depleting the required oxygen concentration and affecting the stoichiometry. Therefore, some hydrogen fractions ignited with 0%, and 25% of the inergen did not combust when 75% of the inergen was introduced.

According to the simulated values shown in Figure 5.3, high LBV and generic battery gas give an absolute maximum explosion pressure of around 800 kPa. However, in the work of Henriksen et al. [13], they obtained maximum explosion pressures of 0.78 and 0.74 MPa (absolute) at the stoichiometry, which is lower than the hydrogen-air mixture done in this study.

High LBV battery gas has 10% CO₂ in its composition, while the generic battery gas has 20.1% CO₂, which has a higher heat capacity than nitrogen and argon. Therefore, battery gas with 100% air should obtain lower explosion pressures than hydrogen with 100% air mixtures because CO₂ has a cooling ability in the reaction.

When inergen is introduced to the flammable mixture, the added inert agents will also contribute to absorbing heat from the reaction, which slows down flame propagation and increases heat losses. Therefore, with the inclusion of inergen, the explosion pressures were reduced for the high LBV battery gases to 584.14 kPa for 50% air and 50% inergen mixture.

Generic battery gases dropped their maximum explosion pressure significantly further with the added inergen than the high LBV battery gas. This is mainly because high LBV has high CO and lower CO₂ fractions than the generic battery gas. From the experiments done by Henrikson et al. [13], 740 kPa maximum explosion pressure was achieved by the generic battery gas combustion in 100% air at 300 K and 1 bar. However, it was reduced to 329.24 kPa maximum explosion pressure with 50% air and 50% inergen.

Both the battery gases did not burn with 75% inergen inclusion in the mixture because, with this amount of inergen, the available air battery gas was minimal, hence the oxygen concentration. High LBV battery gases at stoichiometry levels theoretically need 4.8% O₂, while generic gas needs 4.9% O₂. However, these values are not enough to sustain combustion in hydrocarbon mixtures. Therefore, 75% inergen inclusion will not allow the battery gases to burn.

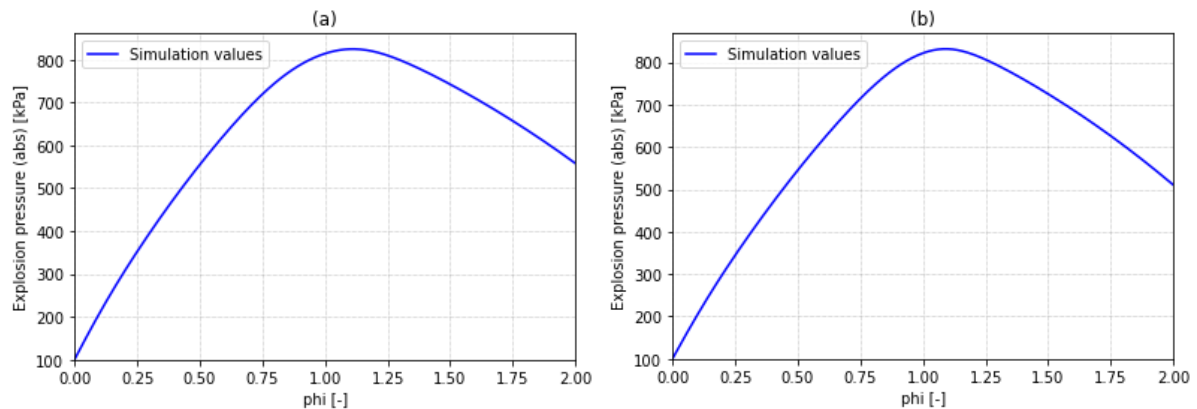


Figure 5.3: Simulated explosion pressures for Battery gases with air using Cantera at 300 K and 1 atm for (a) High LBV battery gas, (b) Generic battery gas

5.3 Maximum rate of explosion pressure rise

As observed in the chapter 4.2.1 $(dp/dt)_{max}$ values were decreased significantly with the addition of inergen, and the highest $(dp/dt)_{max}$ values for almost each sample were recorded near the stoichiometric conditions. With a small flame exposure time, the reaction gives a higher maximum rate of explosion pressure; hence, the reactions with higher burning velocities will obtain a higher maximum rate of explosion pressure. Pure hydrogen has a burning velocity of around 1.85 m/s, while the high LBV battery gas has a velocity of 1.05 m/s and the generic battery gas, 0.5 m/s. Therefore, without the inclusion of inergen, hydrogen will have a higher $(dp/dt)_{max}$ value, which is agreeable with the results. In this experiment for, 100% hydrogen $(dp/dt)_{max}$, the value recorded near stoichiometry is 289.73 MPa/s, whereas Shin [37] obtained a value of around 275 MPa/s. But with the inclusion of inergen, the flammable

mixtures showed a significant reduction in the $(dp/dt)_{max}$ values where the maximum recorded $(dp/dt)_{max}$ for hydrogen with 50% air and 50% inergen was 46.18 MPa/s. This is because inergen reduces the flame temperature by absorbing the heat, and the burning velocity reduces; hence, the low $(dp/dt)_{max}$ values and deflagration index values. Even though the explosion pressure rise rate of the 0.84 equivalence ratio was the highest recorded measure for hydrogen 75% inergen and 25% air mixture which is 0.58 MPa/s, it was not the sample which obtained the highest peak pressure for the sample type. This was because the initial pressure difference, the mixture with 0.81 equivalence ratio had a slightly lower initial pressure than the mixture with 1.25 equivalence ratio.

Furthermore, Henriksen et al. [13], they obtained 81.68 and 32.89 MPa/s $(dp/dt)_{max}$ values for higher LBV battery gas and the generic battery gases at 300 K and 100 kPa. But with the inclusion of inergen, $(dp/dt)_{max}$ values have dropped significantly with values of 6.04 MPa/s for higher LBV battery gas and 0.61 MPa/s with 50% air and 50% inergen.

According to the results obtained, it is appropriate to conclude that introducing inergen can reduce the severity of an explosion by a significant margin.

5.4 How inergen affects the oxygen concentration

As expected, all the maximum explosion pressures recorded for mixtures were near stoichiometry except for the generic battery gas sample with 50% inergen and 50% air. A sample with a 1.03 equivalence ratio obtained a maximum pressure of 291.06 kPa. In contrast, a mixture with an equivalence ratio of 0.81 obtained 329.43 kPa. A reason could be that even though the burnt sample with a 1.03 equivalence ratio was closer to the stoichiometric conditions, it had an oxygen concentration of 9.14. In contrast, the equivalence ratio was 0.81 and had an oxygen concentration of 9.43. As mentioned above, at least 10% oxygen is needed for better combustion of hydrocarbons. Therefore, in this case, the 0.81 equivalence ratio mixture burnt better than the 1.03 equivalence ratio mixture.

Furthermore, as observed in Figure 4.2 where, the richer mixtures did not ignite because when the mixture is on a richer flammable side before inergen inclusion because adding inergen makes the mixture too rich to ignite by reducing the oxygen concentration

As discussed in the literature review, the main fire suppression quality of inergen is to reduce the oxygen concentrations in a mixture in a vessel or a confined area. Figures 5.4 and 5.5 discuss how the stoichiometric oxygen concentration changes with the inclusion of inergen and how the explosion pressure reduces both according to the simulations and the experiments.

In a normal condition, the hydrogen stoichiometric concentration is around 30%. However, with the inclusion of inergen in the mixture, the mixture becomes richer in fuel because of the lack of oxygen in the mixture. Therefore, with inergen, the stoichiometric oxygen concentration drops, as shown in Figures 4.2 (b) and (d); the flammable mixture does not get ignited because of the lack of oxygen in the mixture with 75% of inergen inclusion compared to total inergen and air mixture.

According to Figure 5.5 (left), the limiting oxygen concentration for hydrogen is around 4.5 – 5%. Therefore, the claim that inergen can suppress a fire by reducing the oxygen level to 10–12.5% in the atmosphere is invalid for hydrogen mixtures since it has a lower LOC value than 10%. According to Figure 5.5 (right), no ignition was observed under 8% of oxygen in battery

gas mixtures with inergen; however, the number of experiments carried out with battery gas is insufficient to confirm a LOC value.

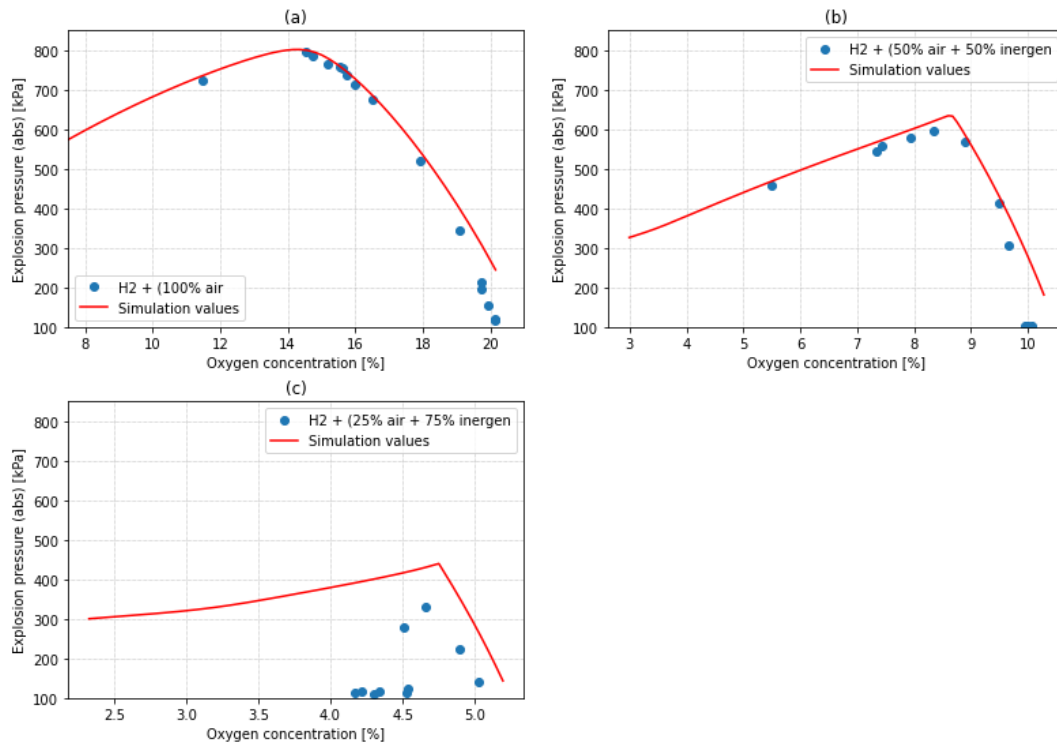


Figure 5.4: Explosion pressure with the oxygen concentration at 1 atm and 300 K for (a) hydrogen with 100 air, (b) hydrogen with 50% air and 50% inergen, (c) hydrogen with 25% air and 75 % inergen.

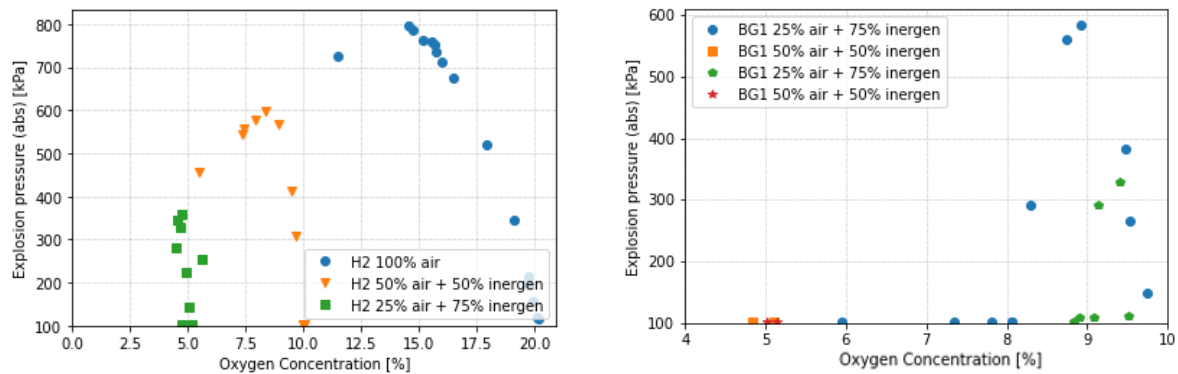


Figure 5.5: Stoichiometric oxygen concentration variation with inergen in hydrogen mixtures (left) and battery gases (right) at 300 K and 1 atm.

5.5 Approximated flammability levels at the NOAEL and LOAEL

As discussed in Chapter 4.3.1, a comparison has been made on the burnt and unburnt samples with a flammability approximation done numerically using the adiabatic temperature. All the samples fit well within and without the flammability limits. Nevertheless, this was done only to get a qualitative idea; therefore, to get more accurate results, it is recommended that experimental results be used.

Figure 5.5 discusses the how inergen performance in the recommended levels of the no observable adverse effects level (NOAEL) and least observable adverse effects level (LOAEL) and the NFPA recommended design concentrations, which were mentioned in the works of Burch et al. [32] Rattananon and Patvichaichod [43].

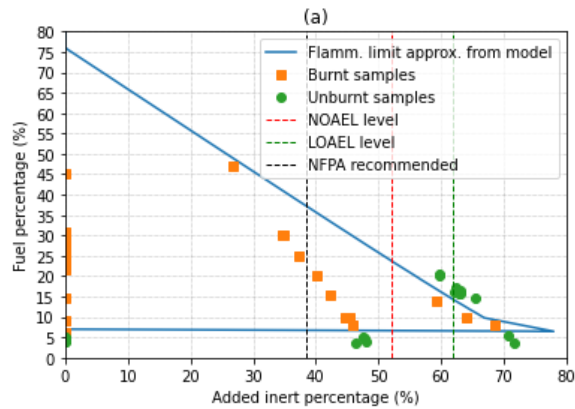


Figure 5.6: Comparison of flammability limits approximation with inergen and the recommended inergen concentrations at 300 K and 1 atm for (a) hydrogen, (b) high LBV battery gas, and (c) generic battery gas.

Table 5.1 summarises the approximated flammability levels that can be achieved at several recommended inergen concentrations in a confined area during an emergency.

Table 5.1: Obtained modified flammability limits with recommended levels [32] [43].

	At NFPA recommendation		At NOAEL value		At LOAEL value	
	LFL (%)	UFL (%)	LFL (%)	UFL (%)	LFL (%)	UFL (%)
Hydrogen	5	37.5	5	23	5	15

6 Future work

Several fire and process safety studies can be built upon this study.

As discussed in this work, explosion characteristics were significantly influenced by inergen. Therefore, studying how the laminar burning velocity varies with inergen for different fuel mixtures is essential.

Ternary diagrams are used to study flammability variations within three-component mixtures: fuel, oxidiser and inert. A study can be done to develop a ternary diagram for inergen for different fuel types, including battery gases and hydrogen. This work can lead to the proposal of a minimum ignition concentration level for the fuels, which would be very useful for industrial applications.

As mentioned in the literature survey above, there are four main clean inert agents at the commercial level: argonite, inergen, carbon dioxide, and argon. A comparison among these inert gases can be conducted to compare which is better for different fire safety scenarios and which is also advantageous for the industry. Furthermore, time is an important parameter when it comes to safety. As discussed in Chapter 2.10.3, inergen has a slower distribution rate than other fire suppressants. Therefore, it will be helpful to compare the effectiveness of inergen with other fire suppressants.

Since hydrogen has a higher ability to detonate, it will be helpful to study how adding an inert gas like inergen can suppress detonation and reduce the possibility of an accident.

As mentioned in the literature survey, it will be difficult to extinguish a fire using only inert gas completely. An investigation can be carried out to study to find our better safety barriers to avoid undesirable circumstances due to thermal runaway in a LIB, including an inert gas like inergen.

7 Conclusion

Diluting flammable mixtures of hydrogen air and LIB vented gases-air using inergen was investigated in this study. Maximum explosion pressure, maximum rate of explosion pressure rise of hydrogen-air-inergen, and LIB vented gases-air were measured in a 20-litre explosion sphere under 300 K and 1 atm with different compositions.

Explosion pressure data of hydrogen and 100% air mixtures showed agreeable results with the Cantera simulations, and the previous studies done. However, with the inclusion of inergen, significant deviations from the simulated values appeared. These inconsistencies may be due to the complexity of the mechanisms with more components and the radiative heat losses with slow flame propagations in the inergen mixed mixtures.

Furthermore, the highest explosion pressures were recorded near the stoichiometric conditions for almost all the mixtures. Hydrogen with 100% air achieved a maximum explosion pressure of 797.46 kPa (absolute) while a maximum rate of explosion pressure rise of 289.73 MPa/s at near stoichiometry. Hydrogen with 50% air and 50% inergen had a maximum explosion pressure of 596.10 kPa (absolute). In comparison, a maximum rate of explosion pressure rise of 46.18 MPa/s at near stoichiometry while a hydrogen mixture with 75% inergen and 25% air obtained a maximum explosion pressure of 253.66 kPa (absolute) while a maximum rate of explosion pressure rise below 1 MPa/s at near stoichiometry. Although high LBV battery gas gave a maximum explosion pressure of 584.34 kPa (absolute) and the generic battery gas, 329.43 kPa (absolute) with 50% air and 50% inergen mixture, the gases did not ignite with 75% inergen and 25% air.

Therefore, it can be established that adding inergen to a flammable mixture can reduce the flammability characteristics by significant margins. However, though inergen claims that it can extinguish fires by reducing the oxygen concentration to 10-12-5%, it didn't apply to hydrogen since it required a minimum around 4.5% oxygen concentration to get ignited.

Furthermore, using their thermodynamic properties, a simple flammability limit variation with an inergen model was developed for hydrogen and battery gases. It showed a satisfactory agreement with the methane propane mixtures in the literature. According to this approximation, 77% of MIC was observed for hydrogen-air-inergen mixtures.

References

- [1] F. Yang *et al.*, “Review on hydrogen safety issues: Incident statistics, hydrogen diffusion, and detonation process,” *Int. J. Hydrog. Energy*, vol. 46, no. 61, pp. 31467–31488, Sep. 2021, doi: 10.1016/j.ijhydene.2021.07.005.
- [2] F. Eljack and M.-K. Kazi, “Prospects and Challenges of Green Hydrogen Economy via Multi-Sector Global Symbiosis in Qatar,” *Front. Sustain.*, vol. 1, p. 612762, Jan. 2021, doi: 10.3389/frsus.2020.612762.
- [3] L. Cai, “Suppression of li-ion battery fires,” Lund University, May 2023.
- [4] “What’s the Best Battery?,” Battery University. Accessed: May 10, 2024. [Online]. Available: <https://batteryuniversity.com/article/whats-the-best-battery>
- [5] S. K. Sharma *et al.*, “Progress in electrode and electrolyte materials: path to all-solid-state Li-ion batteries,” *Energy Adv.*, vol. 1, no. 8, pp. 457–510, 2022, doi: 10.1039/D2YA00043A.
- [6] E. Pawelczyk, N. Łukasik, I. Wysocka, A. Rogala, and J. Gębicki, “Recent Progress on Hydrogen Storage and Production Using Chemical Hydrogen Carriers,” *Energies*, vol. 15, no. 14, p. 4964, Jul. 2022, doi: 10.3390/en15144964.
- [7] “Accidentology involving hydrogen.” Bureau for analysis of industrial risks and pollution.
- [8] H. U. Escobar-Hernandez, R. M. Gustafson, M. I. Papadaki, S. Sachdeva, and M. S. Mannan, “Thermal Runaway in Lithium-Ion Batteries: Incidents, Kinetics of the Runaway and Assessment of Factors Affecting Its Initiation,” *J. Electrochem. Soc.*, vol. 163, no. 13, pp. A2691–A2701, 2016, doi: 10.1149/2.0921613jes.
- [9] V. M. van Essen, *Fundamental limits of NO formation in fuel-rich premixed methane-air flames*. [S.l., [Groningen: s.n.] ; University Library Groningen] [Host], 2007.
- [10] H. Kobayashi, A. Hayakawa, K. D. K. A. Somarathne, and E. C. Okafor, “Science and technology of ammonia combustion,” *Proc. Combust. Inst.*, vol. 37, no. 1, pp. 109–133, 2019, doi: 10.1016/j.proci.2018.09.029.
- [11] C. Dong, Q. Zhou, Q. Zhao, Y. Zhang, T. Xu, and S. Hui, “Experimental study on the laminar flame speed of hydrogen/carbon monoxide/air mixtures,” *Fuel*, vol. 88, no. 10, pp. 1858–1863, Oct. 2009, doi: 10.1016/j.fuel.2009.04.024.
- [12] P. Dirrenberger *et al.*, “Measurements of Laminar Flame Velocity for Components of Natural Gas,” *Energy Fuels*, vol. 25, no. 9, pp. 3875–3884, Sep. 2011, doi: 10.1021/ef200707h.
- [13] M. Henriksen, K. Vaagsaether, J. Lundberg, S. Forseth, and D. Bjerketvedt, “Laminar burning velocity of gases vented from failed Li-ion batteries,” *J. Power Sources*, vol. 506, p. 230141, Sep. 2021, doi: 10.1016/j.jpowsour.2021.230141.
- [14] G. B. Grant and D. Drysdale, *A review of the extinction mechanisms of diffusion flame fires*. London: Home Office, Fire Research and Development Group, 1996.
- [15] S. McAllister, J.-Y. Chen, and A. C. Fernandez-Pello, *Fundamentals of combustion processes*. in Mechanical engineering series. New York: Springer, 2011.

- [16] D. A. Crowl and J. F. Louvar, *Chemical process safety: fundamentals with applications*, 2. ed. in Prentice-Hall international series in the physical and chemical engineering sciences. Upper Saddle River, NJ: Prentice Hall PTR, 2002.
- [17] “Gases - Explosion and Flammability Concentration Limits.” Accessed: May 11, 2024. [Online]. Available: https://www.engineeringtoolbox.com/explosive-concentration-limits-d_423.html
- [18] B. Ma, J. Liu, and R. Yu, “Study on the Flammability Limits of Lithium-Ion Battery Vent Gas under Different Initial Conditions,” *ACS Omega*, vol. 5, no. 43, pp. 28096–28107, Nov. 2020, doi: 10.1021/acsomega.0c03713.
- [19] T. M. H. Le, “Flammability Characteristics of Hydrogen and Its Mixtures with Light Hydrocarbons at Atmospheric and Sub-atmospheric Pressures.” Texas A & M University, Jul. 13, 2013.
- [20] Schroeder, “Explosion Characteristics of Hydrogen-Air and Hydrogen-Oxygen Mixtures at Elevated Pressures,” 2005. [Online]. Available: <https://api.semanticscholar.org/CorpusID:18499929>
- [21] X. Liu and Q. Zhang, “Influence of initial pressure and temperature on flammability limits of hydrogen–air,” *Int. J. Hydrog. Energy*, vol. 39, no. 12, pp. 6774–6782, Apr. 2014, doi: 10.1016/j.ijhydene.2014.02.001.
- [22] “Oxidizing Agents – AFNS Safety.” Accessed: Apr. 30, 2024. [Online]. Available: <https://afns-safety.ualberta.ca/chemical-safety/oxidizing-agents/>
- [23] “Pressure Rise and Explosion Limits.” Accessed: May 02, 2024. [Online]. Available: <https://www.dustlab.eu/en/pressure-rise-and-explosion-limits>
- [24] M. Faghih, X. Gou, and Z. Chen, “The explosion characteristics of methane, hydrogen and their mixtures: A computational study,” *J. Loss Prev. Process Ind.*, vol. 40, pp. 131–138, Mar. 2016, doi: 10.1016/j.jlp.2015.12.015.
- [25] T. Skjold, “Statistics, lessons learnt and recommendations from the analysis of HIAD 2.0 database,” Accessed: May 11, 2024. [Online]. Available: <https://www.clean-hydrogen.europa.eu/system/files/2022-06/Analysis%20of%20hydrogen%20incidents%20and%20accidents%20database%20HIAD%202.0%20%28ID%2013831425%29.pdf>
- [26] D. P. Finegan *et al.*, “Identifying the Cause of Rupture of Li-Ion Batteries during Thermal Runaway,” *Adv. Sci.*, vol. 5, no. 1, p. 1700369, Jan. 2018, doi: 10.1002/advs.201700369.
- [27] T. Lian, “Om Litium-ion batterier og medførende fareaspekter for fritidsfartøy,” Apr. 22, 2021.
- [28] F. Zhao and M. S. Mannan, “Numerical analysis for nitrogen dilution on flammability limits of hydrocarbon mixtures,” *J. Loss Prev. Process Ind.*, vol. 43, pp. 600–613, Sep. 2016, doi: 10.1016/j.jlp.2016.06.015.
- [29] M. Molnarne, P. Mizsey, and V. Schroder, “Flammability of gas mixtures Part 2: Influence of inert gases,” *J. Hazard. Mater.*, vol. 121, no. 1–3, pp. 45–49, May 2005, doi: 10.1016/j.jhazmat.2005.01.033.

- [30] P. J. DiNunno, Society of Fire Protection Engineers, and National Fire Protection Association, Eds., *SFPE handbook of fire protection engineering*, 3. ed. Quincy, Mass: NFPA, National Fire Protection Association, 2002.
- [31] “Inergen gas extraction plant | Fire extinguishing systems AS.” Accessed: May 01, 2024. [Online]. Available: <https://brannsløkkesystemer.no/inergen/>
- [32] I. Burch, S. R. Kennet, and L. E. Fletcher, “A Risk Assessment Approach for Selecting a Replacement for Halon 1301 Fire Suppressant.” DSTO Aeronautical and Maritime Research Laboratory, Mar. 2001.
- [33] Y. Li and J. Yang, “Occupational acute argon gas poisoning: A case report,” *Medicine (Baltimore)*, vol. 101, no. 36, p. e30491, Sep. 2022, doi: 10.1097/MD.00000000000030491.
- [34] “Nitrogen – Hazard and Safeguard!,” May 11, 2024. [Online]. Available: <https://www.aisc.org/ccps/resources/process-safety-beacon/archives/2012/june/english>
- [35] “The Physiology of INERGEN® Fire Extinguishing Agent.” Tyco Fire Protection Products, 2016.
- [36] Y. Jo and D. A. Crowl, “Explosion characteristics of hydrogen-air mixtures in a spherical vessel,” *Process Saf. Prog.*, vol. 29, no. 3, pp. 216–223, Sep. 2010, doi: 10.1002/prs.10370.
- [37] J. Shin, “Hydrogen and ammonia combustion,” University of South-Eastern Norway, Master thesis.
- [38] C.-C. Chen, T.-C. Wang, H.-J. Liaw, and H.-C. Chen, “Nitrogen dilution effect on the flammability limits for hydrocarbons,” *J. Hazard. Mater.*, vol. 166, no. 2–3, pp. 880–890, Jul. 2009, doi: 10.1016/j.jhazmat.2008.11.093.
- [39] L.-Q. Wang, H.-H. Ma, and Z.-W. Shen, “Explosion characteristics of hydrogen-air mixtures diluted with inert gases at sub-atmospheric pressures,” *Int. J. Hydrog. Energy*, vol. 44, no. 40, pp. 22527–22536, Aug. 2019, doi: 10.1016/j.ijhydene.2019.01.059.
- [40] Z. Weiqiang, Z. Shunbing, L. Xun, and H. Xuotong, “Experimental study on suppression of fire and explosion of lithium iron phosphate battery by inert gas,” in *2018 IEEE International Conference of Safety Produce Informatization (IICSPI)*, Chongqing, China: IEEE, Dec. 2018, pp. 57–61. doi: 10.1109/IICSPI.2018.8690468.
- [41] N. Saito, Y. Ogawa, Y. Saso, C. Liao, and R. Sakei, “Flame-extinguishing concentrations and peak concentrations of N₂, Ar, CO₂ and their mixtures for hydrocarbon fuels,” *Fire Saf. J.*, vol. 27, no. 3, pp. 185–200, Oct. 1996, doi: 10.1016/S0379-7112(96)00060-4.
- [42] I. A. Zlochower, “Experimental flammability limits and associated theoretical flame temperatures as a tool for predicting the temperature dependence of these limits,” *J. Loss Prev. Process Ind.*, vol. 25, no. 3, pp. 555–560, May 2012.
- [43] N. Rattananon and S. Patvichaichod, “Performance analysis of inert gas systems in main distribution board room using fire dynamics simulation,” *IOP Conf. Ser. Mater. Sci. Eng.*, vol. 715, no. 1, p. 012006, Jan. 2020, doi: 10.1088/1757-899X/715/1/012006.

Appendices

Appendix A – Signed master's thesis description

Appendix B – Experimental result table

Appendix C – Safety checklist

Appendix D – Flammability limit analysis for battery gases

Appendix E – Python code: Numerical calculation of maximum pressure during the ignition

Appendix F – Python code: Numerical approximation of flammability limits

Appendix G – Balanced chemical reaction for the battery gases and oxygen and air concentrations at different compositions

Appendix A – Signed master's thesis description



Faculty of Technology, Natural Sciences and Maritime Sciences, Campus Porsgrunn

FMH606 Master's Thesis

Title: The Use of Inert Gas for Mitigating Fires and Gas Explosions

Student: Charith Rajapaksha

USN supervisor: Dag Bjerketvedt and Mathias Henriksen

External partner: Equinor and MoZEEs

Task Background: Using inert to mitigate fires and gas explosions is an attractive principle. Low oxygen concentration reduces the reaction rate of the combustion and ultimately quenches the flame. Unfortunately, not only does combustion need oxygen, but humans also need it. An inert gas, therefore, represents a serious hazard by asphyxiation, leading to rapid loss of consciousness and death. Designing and applying an inert gas mitigation system requires detailed knowledge and thorough hazard analysis, or the consequences can be fatal.

Task description:

- Review the effect and the use of inert gas to mitigate fires and gas explosions.
- Perform experiments in the USN 20-liter vessel with low oxygen concentration, hydrogen, and synthetic vent gases from a Li-ion battery.
- Use Cantera to simulate the flame properties of low oxygen concentration, hydrogen, and synthetic vent gases from Li-ion batteries.

Practical arrangements:

Experiments in USN-laboratory Porsgrunn

Supervision:

As a general rule, the student is entitled to 15-20 hours of supervision. This includes the necessary time for the supervisor to prepare for supervision meetings (reading material to be discussed, etc).

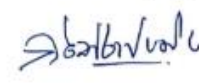
Signatures:

Supervisor (date and signature):

13/5-2024 

Student: Charith Rajapaksha

Student (date and signature):

13/5/2024 

Appendix B – Experimental result table

Hydrogen + 100 % air

test number	initial pressure [mbar]	H2 [mbar]	Air [mbar]	final pressure [mbar]	final temperature [C]	ignition (Y/N)	pressure data	Fuel Conc	Air Conc	O2 Conc	phi [-]	mean p max [kPa]	mean p max abs [kPa]	pepx/pc	pexa/pc	mean dp/dt [MPa/s]	deflagration index [(bar m)/s]
9	100.3	297.6	702.4	1000.0	27.0	Y	Y	29.76	70.24	14.75	1.01	683.52	784.87	6.84	7.85	262.50	717.25
10	101.3	278.0	726.2	1004.2	27.1	Y	Y	27.68	72.32	15.19	0.91	661.95	763.30	6.59	7.60	244.64	668.46
11	100.7	259.8	758.5	1018.3	27.1	Y	Y	25.51	74.49	15.64	0.82	651.92	753.27	6.40	7.40	197.22	538.89
12	101.5	251.0	751.6	1002.6	27.3	Y	Y	25.03	74.97	15.74	0.80	634.47	735.82	6.33	7.34	190.63	520.86
13	101.4	265.2	752.0	1017.2	27.3	Y	Y	26.07	73.93	15.52	0.84	656.75	758.10	6.46	7.45	227.43	621.43
14	97.1	238.5	759.3	997.8	27.3	Y	Y	23.90	76.10	15.98	0.75	611.99	713.34	6.13	7.15	176.70	482.83
15	100.4	215.7	789.3	1005.0	27.3	Y	Y	21.46	78.54	16.49	0.65	574.61	675.96	5.72	6.73	134.13	366.51
16	101.3	146.3	853.0	999.3	27.3	Y	Y	14.64	85.36	17.93	0.41	420.08	521.43	4.20	5.22	27.24	74.44
17	100.7	90.5	910.5	1001.0	27.3	Y	Y	9.04	90.96	19.10	0.24	243.00	344.35	2.43	3.44	1.81	4.94
19	95.3	61.7	947.4	1009.1	26.9	Y	Y	6.11	93.69	19.72	0.16	111.56	212.91	1.11	2.11	1.00	2.74
20	96.8	60.4	940.3	1000.7	27.5	Y	Y	6.04	93.96	19.73	0.15	93.95	195.30	0.94	1.95	0.70	1.90
21	98.4	51.1	955.9	1007.0	26.8	Y	Y	5.07	94.93	19.93	0.13	54.82	156.17	0.54	1.55	0.09	0.25
22	97.9	41.0	963.6	1004.6	27.0	N	Y	4.08	95.92	20.14	0.10	0.00	101.35	0.00	1.01	0.32	0.86
36	98.2	41.2	959.4	1000.6	25.3	N	Y	4.12	95.88	20.14	0.10	0.00	101.35	0.00	1.01	0.09	0.24
37	99.5	313.9	702.8	1016.7	26.9	Y	Y	30.87	69.13	14.52	1.06	696.11	797.46	6.85	7.84	289.73	791.66
48	97.3	459.2	553.5	1012.7	27.1	Y	Y	45.34	54.66	11.48	1.98	622.79	724.14	6.15	7.15	255.80	698.96

Hydrogen + (50 % air + 50 % inergen)

test number	initial pressure [mbar]	H2 [mbar]	INERGEN [mbar]	final pressure [mbar]	final temperature [C]	igniter	ignition (Y/N)	pressure data	Fuel Conc	Inergen Conc	O2 Conc	phi [-]	mean p max [kPa]	mean p max abs [kPa]	pepx/pc	pexa/pc	mean dp/dt [MPa/s]	Mean deflagration index [(bar m)/s]	sigma		
23	98.4	303.0	350.3	1010.9	27.0	wire	Y	Y	29.97	34.65%	7.43	2.02	455.06	556.41	4.50	5.50	35.42	1.55	96.77	4.62	
24	99.6	303.8	349.4	1003.5	27.2	wire	Y	Y	30.27	34.82%	7.33	2.06	444.11	545.46	4.43	5.44	33.68	1.53	92.03	4.58	
26	100.8	252.2	376.3	1010.9	27.2	wire	Y	Y	24.95	37.22%	7.94	1.57	475.86	577.21	4.71	5.71	44.02	1.64	120.28	4.84	
27	100.0	155.0	426.8	1010.3	27.2	wire	Y	Y	15.34	42.24%	8.91	0.86	465.66	567.01	4.61	5.61	24.24	1.38	66.23	4.76	
28	98.0	202.9	402.2	1004.1	27.5	wire	Y	Y	20.21	40.06%	8.34	1.21	494.75	596.10	4.93	5.94	46.18	1.66	126.18	5.02	
29	94.7	100.5	450.2	1004.7	28.1	wire	Y	Y	10.00	44.81%	9.49	0.53	310.99	412.34	3.10	4.10	2.76	0.44	7.53	3.58	
31	94.5	80.8	460.9	1003.4	27.6	wire	Y	Y	8.05	45.93%	9.66	0.42	205.64	306.99	2.05	3.06	0.40	-0.40	1.10	3.12	
32	97.9	51.5	475.4	1002.0	27.3	wire	N	Y	5.14	47.45%	9.96	0.26	0.00	101.35	0.00	1.01	0.10	-1.02	0.26	2.40	
33	97.8	41.4	479.9	1000.8	27.1	wire	N	Y	4.14	47.95%	10.06	0.21	0.00	101.35	0.00	1.01	0.14	-0.86	0.38	2.14	
34	98.6	46.2	478.3	1001.7	27.1	wire	N	Y	4.61	47.75%	10.00	0.23	0.00	101.35	0.00	1.01	0.16	-0.79	0.45	2.26	
35	97.0	37.0	482.3	1042.5	25.8	wire	Y	Y	3.55	46.26%	10.54	0.17	0.00	101.35	0.00	0.97				1.98	
30	99.7	103.8	471.1	1035.6	27.6	wire	Y	Y	10.0	45.49%	9.34	0.54	298.85	400.20	2.89	3.86					
47	97	498	281.5	1055.4	27.2	wire	Y	Y	47.2	26.67%	5.49	4.30	356.39	457.74	3.38	4.34					

Hydrogen + (25 % air + 75 % inergen)

test number	initial pressure [mbar]	H2 [mbar]	INERGEN [mbar]	final pressure [mbar]	final temperature [C]	igniter	ignition (Y/N)	pressure data	Fuel Conc	Inergen Conc	O2 Conc	phi [-]	p1 max [kPa]	p2 max [kPa]	mean p max [kPa]	mean p max abs [kPa]	pepx/pc	pexa/pc	mean dp/dt [MPa/s]	deflagration index [(bar m)/s]	sigma	comments	
38	97.6	202.3	600.7	1004.9	27.1	wire	N	Y	20.13	59.78	4.22	2.39	15.08	13.19	14.14	101.33	0.14	0.67	2.48				
40	98.3	108.3	681.2	1005	27	wire	Y	Y	9.98	63.86	4.86	1.04	224.09	291.20	227.85	328.97	2.14	1.88	3.59				
41	92.4	205.8	600.5	1006.3	27.2	wire	N	Y	20.45	59.67	4.17	2.45	13.16	8.41	10.79	101.33	0.11	0.43	2.47				
42	97.3	93.5	714.3	1009.7	27.2	wire	N	Y	5.30	70.74	5.03	0.53	39.12	41.39	40.26	101.33	0.40		2.03				
43	96.3	37.1	727.9	1014.9	27.2	wire	N	N	3.66	71.72	5.17	0.35	[-]	[-]	[-]	101.33	#VALUE!	1.68	3.21				
45	60	158.7	640.5	1019.7	27.1	wire	Y	Y	15.56	62.81	4.54	1.71	23.25	18.33	20.79	101.33	0.20	2.67	3.38				
46	96.8	177	645.2	1036.1	27.3	wire	Y	Y	17.08	62.27	4.34	1.97	14.12	13.17	13.65	101.33	0.13						
49	95.2	150.1	670.1	1025.1	27.3	wire	N	N	14.64	65.37	4.20	1.74	[-]	[-]	[-]	101.33	#VALUE!						
51	97.5	160.1	641.7	1018	27.3	wire	N	N	15.73	63.04	4.46	1.76	[-]	[-]	[-]	101.33	#VALUE!						
52	97.3	82.7	691.9	1010.2	27.2	wire	Y	Y	8.19	68.49	4.90	0.84	120.25	125.06	122.66	223.98	1.21						
53	93.1	142.9	603.4	1019.2	27.2	wire	Y	Y	14.02	59.20	5.62	1.25	147.63	157.05	152.34	253.66	1.49						
54	94	164	630	1012.1	28.3	wire	N	Y	16.20	62.25	4.53	1.79	15.14	10.71	12.92	101.33	0.13						
55	93.6	200.5	766.4	1215.7	27	wire	N	Y	16.49	63.04	4.30	1.92	10.41	7.83	9.12	101.33	0.08						

High LBV BG + (50 % air + 50 % inergen)

name of experiment	initial pressure [mbar]	H2 [mbar]	INERGEN [mbar]	final pressure [mbar]	final temperature [C]	igniter	ignition (Y/N)	pressure data	Fuel Conc	Inergen Conc	with air and inergen	O2 Conc	phi [-]	mean p max [kPa]	mean p max abs [kPa]	pepx/pc	pexa/pc	mean dp/dt [MPa/s]	deflagration index [(bar m)/s]	sigma	
445.5	285.0	1019.3	27.0	wire	N	N	43.71	27.96	0.50	5.95	4.64	0.00	101.35	0.00	0.99	[-]	[-]			3.31	
147.4	436.4	1015.8	27.2	wire	Y	Y	14.51	42.96	0.50	8.93	1.03	483.01	584.34	4.76	0.78	6.04	16.49	4.46			
212.0	418.4	1040.0	27.3	wire	Y	Y	20.38	40.23	0.51	8.27	1.56	382.48	483.83	3.68	4.65	2.11	5.75	4.76			
102.6	450.9	1008.7	27.4	wire	Y	Y	10.17	44.70	0.50	9.48	0.68	280.28	381.63	2.78	3.78	1.04	2.85	4.19			
85.5	467.4	1012.4	27.3	wire	Y	Y	8.45	46.17	0.50	9.53	0.56	164.18	265.53	1.62	2.62	0.58	1.58	3.72			
70.9	470.6	1010.6	27.3	wire	Y	Y	7.02	46.57	0.50	9.75	0.45	47.23	148.58	0.47	1.47	0.21	0.58	3.30			
302.7	354.0	1009.8	27.3	wire	N	N	29.98	35.06	0.50	7.34	2.58	0.00	101.35	0.00	1.00	[-]	[-]	4.14			
256.3	379.2	1012.1	27.3	wire	N	N	25.32	37.47	0.50	7.81	2.05	0.00	101.35	0.00	1.00	[-]	[-]	4.45			
227.6	402.0	1033.2	27.2	wire	Y	Y	22.03	38.91	0.50	8.20	0.00	359.22	460.57			1.44	3.92	4.69			
252.9	378.4	1024.7	27.4	wire	N	N	24.68	36.93	0.49	8.06	1.93	0.00	101.35	0.00	0.99	[-]	[-]	4.57			
236.6	389.3	1015.8	27.6	wire	N	N	23.29	38.32	0.50	8.06	1.62	0.00	101.35	0.00	1.00	[-]	[-]	4.60			
164.3	427.6	1013.4	27.2	wire	Y	Y	16.21	42.19	0.50	8.73	1.17	458.86	560.21	4.53	5.53	5.71	15.60	5.08			
217.7	528.7	1340.0	27.2	wire	Y	Y	0.00	39.46	0.47	12.71	1.10	622.44	0.00	4.65	0.00	9.86	26.94	5.31			
218.8	393.7	1012.9	27.2	wire	Y	Y	21.60	38.87	0.50	8.30	1.64	189.45	290.80	1.87	2.87	0.24	0.65	4.75			

High LBV BG + (75 % air + 25 % inergen)

name of experiment	initial pressure [mbar]	H2 [mbar]	INERGEN [mbar]	final pressure [mbar]	final temperature [C]	igniter	ignition (Y/N)	pressure data	Fuel Conc	Inergen Conc	O2 Conc	phi [-]	mean p max [kPa]	mean p max abs [kPa]	mean dp/dt [MPa/s]	deflagration index [(bar m)/s]					
70	95.9	81.2	697.4	1011.5	27.4	wire	N	N	8.03	68.95	4.84	1.05		0.00		101.33	[-]	[-]			
71	96.7	72.5	712.8	1037.3	27.0	wire	N	N	7.00	68.72	5.10	0.87		0.00		101.33	[-]	[-]			

Generic LBV BG + (50 % air + 50 % inergen)

test number	initial pressure [mbar]	H2 [mbar]	INERGEN [mbar]	final pressure [mbar]	final temperature [C]	igniter	ignition (Y/N)	pressure data	Fuel Conc	Inergen Conc	O2 Conc	phi [-]	mean p max [kPa]	mean p max abs [kPa]	pexg/pC	pexa/pC	mean dp/dt [MPa/s]	Mean dp/dt [log (m/s)]	ion index [bar]	sigma
75	97.8	127.4	446.2	1015.8	27.1	wire	Y	Y	12.54	43.93	9.14	1.03	189.73	291.06	1.87	2.87	0.31	-0.51	0.85	5.10
76	95.6	200.5	401.9	1040.0	27.2	wire	N	N	19.28	38.64	8.84		0.00	101.33	0.00	0.00				4.65
77	96.8	158.4	432.0	1024.8	27.1	wire	N	Y	15.46	42.15	8.90	1.30	7.46	108.79	0.07	1.06	0.03	-1.54	0.08	4.85
78	95.9	102.8	456.8	1014.4	27.2	wire	Y	Y	10.13	45.03	9.42	0.81	228.11	329.43	2.25	3.25	0.61	-0.22	1.66	4.52
79	92.0	132.1	435.0	1037.0	27.3	wire	N	Y	12.74	41.95	9.52		9.28	110.60	0.09	1.07			0.54	5.25
80	94.0	133.1	438.7	1007.5	27.2	wire	N	Y	13.21	43.54	9.08	1.09	8.50	109.82	0.08	1.09	0.16	-0.80	0.44	5.04

Generic LBV BG + (25 % air + 75 % inergen)

test number	initial pressure [mbar]	H2 [mbar]	INERGEN [mbar]	final pressure [mbar]	final temperature [C]	igniter	ignition (Y/N)	pressure data	Fuel Conc	Inergen Conc	O2 Cor	phi [-]	mean p max [kPa]	mean p max abs [kPa]	mean dp/dt [MPa/s]	deflagrat ion index [bar]	sigma
81	80.4	69.6	703.9	1015.9	27.2	wire	N	N	6.85	69.29	5.01	1.02	0.00	101.33	[-]	[-]	[-]
82	97.6	54.2	713.2	1016.5	27.2	wire	N	N	5.33	70.16	5.15	0.78	0.00	101.33	[-]	[-]	[-]

Appendix C – Safety checklist

Safety checklist and results matrix for explosion sphere experiments.

Date:

Project Number:

01 – Protection gear	06 – Check Air compressor or outlet	
02 – Check fire extinguisher	07 – Start all sensors and the explosion sphere	
03 – Start ventilation	07 – Start data acquisition systems	
04 – Check state of explosion sphere	09 – Tighten explosion sphere lid.	
05 – Prepare gas cylinder /chemical	10 – Start the heating system	

Note: All valves are all valves except v1 and v2 (the valves for heating cap).

Name of experiment					
Time					
Type of fuel					
Concentrations	Fuel				
	Air				
	Inert				
Set igniting cable					
Close all valves and the sphere					
Open V3 and V4					
Set vessel temperature					
Start ambient pressure logger					
Start stirrer & vacuum pump					
Close V3 at desired pressure					
Stop stirrer & vacuum pump					
Initial Pressure					
Add Fuel					
Partial Pressure with Fuel					
Add Inert					
Partial Pressure with Inert					
Start stirrer					
Add oxidizer					
Start timer (5 min)					
Stop stirrer					
Start timer (3 min)					
End Temperature					
Final Pressure					
Close V4					
Stop ambient pressure logger					
Check that all valves are closed					
Connect igniter					
Check amplifiers					
Oscilloscope in the single mode					
Ignite mixture					
Ignition (Yes/No)					
Disconnect igniter					
Start Fume extractor					
Open V6 and V5					
Flush system (5 min)					
Close V6 and B5					
Stop fume extractor					
Save all data					

01 – Shut down compressor and make delP.0	04 – Turn off dryer	
02 – Shut down computers	05 – Open explosion sphere lid	
03 – Turn off explosion sphere	06 – Stop ventilation	

Comments:

Remember to write any comments or remarks in the [logbook](#)

Appendix D – Simple flammability limit analysis for battery gases

A similar approximation for hydrogen with inergen was applied to high LBV battery gas and the generic battery gas mixtures, as shown in Figures A and B. As expected, high LBV battery gas showed a wider flammability range than the generic battery gas. The MIC level for flammable mixtures at atmospheric conditions was around 68% and 55% inergen into the total mixture. All the unburnt samples in both gases were fitted outside except one sample for generic battery gas, which was fitted closer to the flammability range. All the burnt samples were fitted into the flammability limit approximation as required.

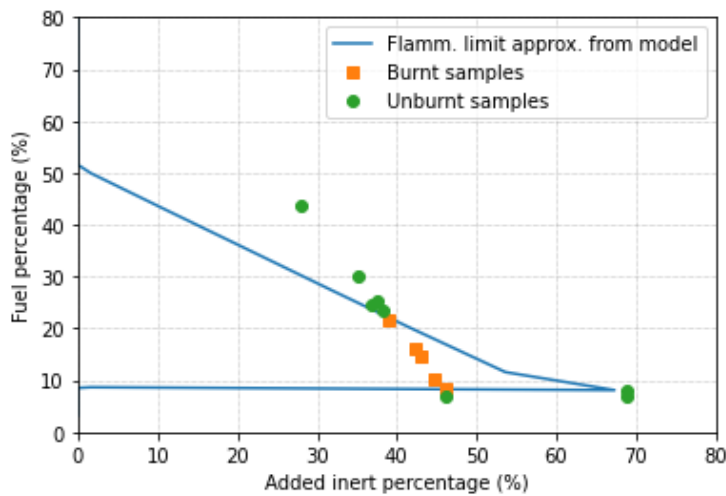


Figure A: Numerical approximation for flammability variation for high LBV battery gas with inergen added, with burnt and unburnt samples given.

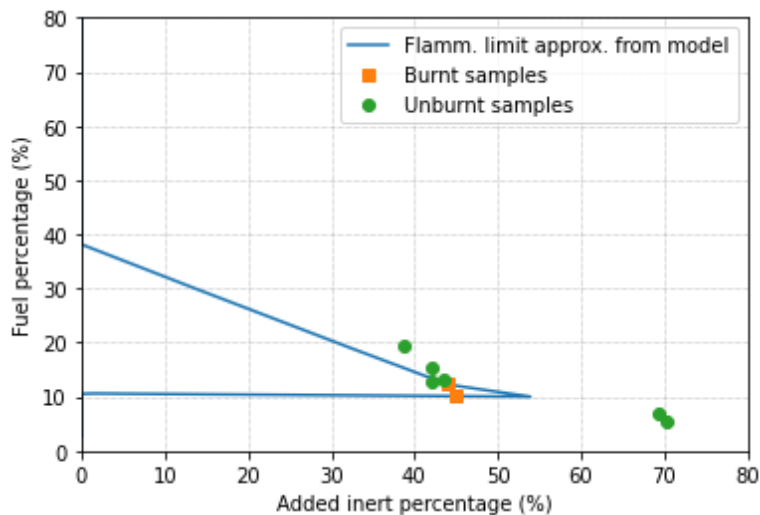


Figure B: Numerical approximation for flammability variation for generic battery gas with inergen added, with burnt and unburnt samples given.

Appendix E – Python code: Numerical calculation of maximum pressure during the ignition

```
# -*- coding: utf-8 -*-
"""
Created on Tue May 7 20:27:13 2024

@author: chari
"""

#import os
import pandas as pd
#import cantera as ct
import matplotlib.pyplot as plt
#print (os.getcwd())
import cantera as ct
import numpy as np

def calculate_pressure(phi_s,phi_f,fuel,oxidizer,reactionMech='gri30.yaml'):
    phi = np.arange(phi_s, phi_f, 0.01)
    size = len (phi)
    pressure_array = np.zeros(size)
    conc_array = np.zeros(size)
    p = 1e5 # pressure [Pa], 101325 is one atm
    Tin = 300.0 # unburned gas temperature [K]
    "define fuel and oxidizer separatly as described in the equivalence ratio tutorial,"
    for equ in range (0,size):
        # Solution object used to compute mixture properties
        #mygas = ct.Solution(reactionMech)
        mygas = ct.Solution("gri30.yaml")
        mygas.set_equivalence_ratio(phi[equ], fuel, oxidizer)
        mygas.TP = Tin, p
        xH2=mygas['H2'].X[0]
        #xFuel=mygas.X[0]/0.428
        #print(xFuel)
        mygas.equilibrate( "UV")
        # Set up flame object
        #print (mygas.P)
        pressure_array[equ] = mygas.P/1000
        conc_array[equ] = xH2*100
    plt.plot(conc_array,pressure_array)
    #write2ex(phi,pressure_array,1,2,'output_BG2.xlsx')
    #print(pressure_array)
```

```

#print(phi)
df = pd.read_excel('Result table.xlsx',sheet_name='Hydrogen 75')
conc = (df['Fuel Conc.'])
df = pd.read_excel('Result table.xlsx',sheet_name='Hydrogen 75')
mean_pres = (df['mean p max abs [kPa]'])

plt.plot(conc,mean_pres, 'o',label='Experimental values')
plt.plot(conc_array,pressure_array,'red', label='Simulation values')

plt.xlabel('Fuel Concentration (%)')
plt.ylabel('Explosion pressure (abs)')
#plt.legend(['Simulation values','Experimental values'])
plt.legend(loc='lower right')
plt.grid(True, which='major', linestyle=':', linewidth=0.5, color='gray')
plt.xlim(xmin=0.0)
plt.ylim(ymin=100.0,ymax=850)
plt.legend(loc='best')
#plt.xlim([0, x_max])
#plt.ylim([0, y_max])
#ax = plt.gca()
#ax.spines['left'].set_position(('data', 0))
#ax.spines['bottom'].set_position(('data', 0))
#ax.xaxis.set_ticks_position('bottom')
#ax.yaxis.set_ticks_position('left')
return pressure_array
return conc_array
return phi

fuel = "H2:1"
#fuel = "H2:0.428, CO:0.371, CO2:0.10, CH4:0.071 C2H4: 0.03" #Battery Gas 1 High LBV
#fuel = "H2:0.349, CO:0.250, CO2:0.201, CH4:0.150 C2H4: 0.05" #Battery Gas 2 Generic gas

#oxidizer ="O2:0.105, N2:0.655, Ar:0.2, CO2:0.04" # or ="O2:1,N2:"+str(79/21) INERGEN 50%
oxidizer ="O2:0.0525, N2:0.5875, Ar:0.3, CO2:0.06" # or ="O2:1,N2:"+str(79/21) INERGEN 75%
#oxidizer = 'O2:0.21, N2:0.79'+str(79./21.)

calculate_pressure(0.1,2.5,fuel,oxidizer)

```

Appendix F – Python code: Numerical approximation of flammability limits

```
# -*- coding: utf-8 -*-
"""
Created on Tue May 14 20:46:48 2024

@author: chari
"""

import cantera as ct
import numpy as np
import matplotlib.pyplot as plt
import pandas as pd

gas = ct.Solution('gri30.yaml')

#fuel = "H2:0.428, CO:0.371, CO2:0.10, CH4:0.071 C2H4: 0.03" #Battery Gas 1 High LBV
fuel = "H2:0.349, CO:0.250, CO2:0.201, CH4:0.150 C2H4: 0.05" #Battery Gas 2 Generic gas
#fuel = 'CH4:1'

oxidizer = 'O2:0.21, N2:0.79'
diluent = 'Ar:0.4, CO2:0.08, N2:0.52'

dil = 0
fuelConcentrationList=list()
diluentConcentration=list()
TList=list()
rangeOfPhi1 = list(np.arange(0.1,1,0.01))
rangeOfPhi2 = list(np.arange(1,14.5,0.1))
rangeOfPhi =rangeOfPhi1 + rangeOfPhi2

for phi in rangeOfPhi1:
    while dil < .85:
        gas.set_equivalence_ratio(phi, fuel , air, diluent=diluent, fraction={"diluent":
dil})

        gas.TP= 300, 101325
        xH2=gas['H2'].X[0]/0.349
        gas.equilibrate( "HP") # "UV" is a string
        if gas.T >= 1200:
            dil = dil + 0.001
        if gas.T <= 1200:
            xH2perc = xH2 * 100
            dilperc = dil * 100
```

```

        fuelConcentrationList.append(xH2perc)
        diluentConcentration.append(dilperc)
        TList.append(gas.T)
        dil=0
        break
for phi in rangeOfPhi2:
    while dil < .85:
        gas.set_equivalence_ratio(phi, fuel , air, diluent=diluent, fraction={"diluent":
dil))

        gas.TP= 300, 101325
        xH2=gas['H2'].X[0]/0.349
        gas.equilibrate( "HP") # "UV" is a string
        if gas.T >= 1650:
            dil = dil + 0.001
        if gas.T <= 1650:
            xH2perc = xH2 * 100
            dilperc = dil * 100
            fuelConcentrationList.append(xH2perc)
            diluentConcentration.append(dilperc)
            TList.append(gas.T)
            dil=0
            break

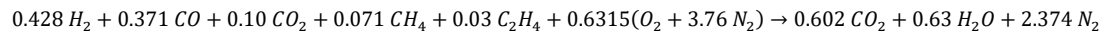
df_BG2 = pd.read_excel('Result table.xlsx',sheet_name='BG2_Flam')
conc_BG2_flam = (df_BG2['ffc'])
conc_BG2_Inert_flam = (df_BG2['fic'])
df_BG2_no_ = pd.read_excel('Result table.xlsx',sheet_name='BG2_Flam')
conc_BG2_flam_no = (df_BG2_no_['nfc'])
conc_BG2_Inert_no = (df_BG2['nic'])

plt.plot(diluentConcentration,fuelConcentrationList,label='Flamm. limit approx. from model')
plt.plot(conc_BG2_Inert_flam,conc_BG2_flam,'s',label='Burnt samples')
#plt.plot(conc_H2_75_Inert_flam,conc_H2_75_flam, 'o')
plt.plot(conc_BG2_Inert_no,conc_BG2_flam_no, 'o',label='Unburnt samples')
#plt.axvline(x=52, color='r', linestyle='--', linewidth=1, label='NOAEL level')
#plt.axvline(x=62, color='g', linestyle='--', linewidth=1, label='LOAEL level')
#plt.axvline(x=38.5, color='black', linestyle='--', linewidth=1, label='NFPA recommended')
plt.xlim(xmin=0.0,xmax=80)
plt.ylim(ymin=0.0, ymax=80)
plt.xlabel('Added inert percentage (%)')
plt.ylabel('Fuel percentage (%)')
plt.title('(b)')
plt.legend(loc='upper right')
plt.grid(True, which='major', linestyle=':', linewidth=0.5, color='gray')

```

Appendix G – Balanced chemical reaction for the battery gases and oxygen and air concentrations at different compositions

High LBV battery gas reaction with air



Generic battery gas reaction with air

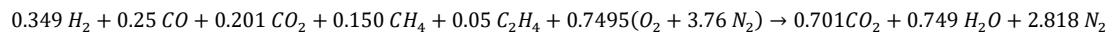


Table A: Required air and oxygen concentrations for different mixtures at stoichiometry.

Component	Air concentration at stoichiometry	O2 concentration at stoichiometry
High LBV BG + 100 %	75 %	15.76 %
High LBV BG + (50 % + 50% inergen)	42.9%	9%
High LBV BG + (25 % + 75% inergen)	23%	4.8%
Generic BG + 100 %	73.8%	15.5%
Generic BG + (50 % + 50% inergen)	42.5%	8.9%
Generic BG + (25 % + 75% inergen)	22.9%	4.8%